SAPIENZA
Università di Roma
Facoltà di Scienze Matematiche Fisiche e Naturali

DOTTORATO DI RICERCA
IN BIOLOGIA CELLULARE E DELLO SVILUPPO

PH. D. IN CELL AND DEVELOPMENTAL BIOLOGY

Ciclo/Cycle: XXXI
(A.A. 2017/2018)

Mitochondria and metabolism: the role of SAGA complex in budding yeast respiration

Dottorando/Ph. D. Student
Manuela Leo

Docente guida/Supervisor
Prof. Silvia Francisci

Coordinatore/Coordinator
Prof. Giulia De Lorenzo

Index

Sommario

Il mitocondrio è un organello cellulare dotato di un proprio DNA e di un proprio macchinario di sintesi proteica. E' responsabile di diversi processi metabolici, tra cui la respirazione cellulare, che comporta la produzione molecole di ATP e quindi di energia. Le funzioni mitocondriali sono fondamentali per l'omeostasi della cellula. Questo determina una continua comunicazione tra nucleo e mitocondrio con modificazioni dei livelli trascrizionali dei prodotti coinvolti. I meccanismi epigenetici, in particolare l'acetilazione, sono responsabili delle modifiche post-traduzionali sia delle proteine istoniche che degli enzimi di diverse vie metaboliche. Il lievito è un ottimo modello cellulare per lo studio dei meccanismi epigenetici associati ai cambiamenti metabolici. In questo organismo è possibile confrontare cellule che respirano con cellule che fermentano semplicemente variando la fonte di carbonio nel terreno di crescita. Il complesso SAGA è un attivatore trascrizionale altamente conservato che presenta due moduli con attività catalitica: il domino HAT con l'acetiltransferasi Gcn5 e il modulo DUB con la deubiquitinasi Ubp8. Nel mio lavoro di dottorato ho studiato il coinvolgimento di SAGA nella respirazione. I risultati mostrano che l'integrità del complesso e le sue attività catalitiche sono necessarie per la crescita in un mezzo di coltura unicamente respirabile. Inoltre, i livelli di espressione di Gcn5 e di Ubp8 aumentano notevolmente nel passaggio dalla fermentazione alla respirazione. Ho dimostrato che in cellule che respirano l'E3 ubiquitina ligasi Psh1 e la HDAC Hda1 sono interattori funzionali di Ubp8 e Gcn5. Hda1, in particolare, risulta avere una attività opposta a quella di Gcn5 nella acetilazione del residuo istonico H3K18. Infine, i miei risultati indicano che Gcn5, Ubp8 e Psh1 localizzano non solo nel nucleo, ma anche nei mitocondri indipendentemente dal complesso SAGA. Questi dati evidenziano una nuova funzione per questi enzimi epigenetici e dimostrano un importante ruolo come regolatori delle dinamiche mitocondriali.

Summary

Mitochondrion is the energy centre of the cell in which different metabolic pathways converge. Cell respiration takes place in this organelle with high production of ATP. Nucleus-mitochondrion communication represents an essential level of cell homeostasis regulation. This crosstalk is strictly related to epigenetic mechanisms, in particular to histone and non-histone proteins acetylation. Budding yeast is a suitable model system to study the interplay between epigenetic and metabolism; in this organism it is possible to analyse fermentative and respiratory pathways varying the carbon source in growth medium. SAGA complex is a transcriptional co-activator with two catalytic domains: the deubiquitination module with DUB Ubp8 and the acetylation domain with HAT Gcn5. In yeast, Gcn5 has a major role in protein acetylation at global and specific lysine; moreover, it is implicated in mitochondrion-nucleus communication. In this work, we found that SAGA complex and its catalytic activities are necessary for cell respiration. Results showed that KAT Gcn5 and DUB Ubp8 are upregulated in respiration at both transcriptional and protein levels. We identify two interactors, the E3 ubiquitin ligase Psh1 and the HDAC Hda1, whose deletion is able to rescue defective respiratory phenotype of strains lacking respectively Ubp8 and Gcn5. We demonstrated that histone residue H3K18 is the preferential target of Hda1 and Gcn5 and its acetylation is needed in respiration. Surprising, we found that Gcn5, Ubp8 and Psh1 localize in both nucleus and mitochondria highlighting a dual role as chromatin modifiers and mitochondrial factors. Moreover, our data showed that Ubp8 expression is regulated by Gcn5, while its cell localization is influenced by Psh1. Finally, results suggest that acetylation is an important mark in respiratory condition.

Introduction

Epigenetic is the study of heritable changes in gene function that do not involve alteration of DNA sequence. More in general, epigenetic refers to the mechanisms that regulate gene expression in cell cycle progression and that maintain cell identity during mitotic/meiotic division. A well-studied mechanism is the reversible post-translational modification (PTM) of histones, protein core of nucleosomes and chromatin in Eukaryotes (Moore, 2017). Histone modifications occur through the addition of various chemical groups, as methyl and acetyl moieties, with consequences in chromatin condensation and transcription factors recruitment. One of the most studied PTM is acetylation of histone lysine that leads to chromatin relaxation, associated to transcription activation (Graff and Tsai, 2013). A PTM with multiple roles is ubiquitination. Ubiquitin is a 76 amino acids peptide that binds lysine residues of histones H2A and H2B with effect on transcription activity (Rothbart and Strahl, 2014). In non-histone proteins, ubiquitination is mainly involved in protein localization, activation and targeting to degradation through proteasomal system (Park and Ryu, 2014). The enzymes that add or remove these groups on specific histone and non-histone proteins are often found in multi-protein complex. SAGA (Spt–Ada–Gcn5 acetyltransferase) is a transcriptional coactivator complex highly conserved from yeast to human and organized in functional/structural modules. In yeast, it is composed of a recruitment domain with Tra1, a TBP interaction unit containing Spt3 and Spt8, an architecture domain (Spt7, Spt20, Ada1, TAF5, -6, -9 and -12) and two units with catalytic activity: the acetylation (Gcn5, Ada2, Ada3) and the deubiquitination (Ubp8, Sus1, Sgf11 and Sgf73) modules (Koutelou et al., 2010). KAT Gcn5 carries out the acetylation activity. This KAT has a major role in histone H3 acetylation at genome-wide levels and at specific loci linked to stress response. Moreover, it was found to bind promoter and 5' coding regions of most highly transcribed genes (Koutelou et al., 2010). The second catalytic module of SAGA is the deubiquitination domain with DUB Ubp8. This enzyme removes ubiquitin molecules from histone H2B with

effects on transcription activation and transition to elongation (Henry et al., 2003, Wyce et al., 2007). Ubp8 has been shown to acts also in non-histone protein deubiquitination. One target is the yeast protein kinase Snf1, homologue of human AMPK. Snf1 is a regulator of growth in presence of low glucose or alternative carbon sources and it is required for response to environmental and nutritional stress (Hsu et al., 2015). In Mammalia, SAGA is involved in crucial processes, including embryonic development, stress responses, cell growth, genome integrity and metabolic control (Wang and Dent, 2014). SAGA and Gcn5 have been reported to interact with the oncoprotein Myc and are required for activation of Myc target genes (Martinez-Cerdeno et al., 2012). Moreover, Gcn5 has a role in acetylation of the tumor suppressor p53, with effects on the transcription of its target genes (Barlev et al., 2001). These findings highlight a possible role of Gcn5 in cancer growth. For example, Gcn5 is highly expressed in non-small-cell lung cancers in which it enhances cell growth (Chen et al., 2013). In past, Usp22, homologous of yeast Ubp8, has been identified as part of an 11-gene 'death from cancer' signature for highly aggressive and therapy resistant tumors (Glinsky, 2005). Several studies have confirmed the role of Usp22 as oncogene, regulating cell cycle progression, proliferation and apoptosis. Increased expression of Usp22 was linked to poor prognosis in several cancers, such as liver, colorectal and breast cancers (Wang and Dent, 2014).

Studying the pathways related to normal cell growth and proliferation is fundamental to understand mechanisms mis-regulated in disease. For this purpose, the budding yeast *S. cerevisiae* is a useful model system. It is a single-cell eukaryote with the 30% of genes homologous to human ones (Heinicke et al., 2007). The yeast genome was the first eukaryotic DNA that has been sequenced and a large numbers of genetic and functional databases and –omics resources are now available. *S. cerevisiae* is a suitable tool for genetic and molecular studies due to its rapid time of duplication and the possibility to create knock out strains in specific loci using homologous recombination. The budding yeast can growth in both aerobic and anaerobic conditions and the choice between

fermentation (anaerobic) and respiration (aerobic) depends on carbon sources availability. In presence of high levels of glucose *S. cerevisiae* produces ethanol via fermentation (Crabtree effect), while in presence of low glucose or alternative carbon sources respiration is the preferential pathway (Otterstedt et al., 2004). This is a big advantage in metabolic studies, because it is possible to induce respiration or fermentation simply varying the carbon source in growth medium.

The switch between fermentation and respiration causes important changes in expression of genes involved in catabolic pathways, ribosomal biogenesis and stress response (Broach, 2012). These changes occur through epigenetic mechanisms, in particular by reversible post-translational modifications (PTMs) of histone and non-histone proteins. Protein acetylation plays a major role in regulation of metabolism modulating the activation of metabolic genes. Moreover, most of the proteins of catabolic network are regulated by acetylation/deacetylation, including the enzymes of glycolysis and TCA cycle (Baeza et al., 2016) (Guan and Xiong, 2011). Among other post-translational modification that affects metabolic regulation, there is the addition of ubiquitin molecules. Ubiquitination is required for activation of metabolism regulators as Akt and AMPK (Yang et al., 2009). Moreover, deficiency in ubiquitination system has been associated to deregulation of glucose uptake and glycolysis (Chan et al., 2012). Respiration takes place in mitochondrion, an organelle possessing its own DNA and regulated by both nuclear and mitochondrial genomes. Nucleus controls mitochondrion activity through the "anterograde response" with effects on its functions and biogenesis (Quiros et al., 2016). This regulation occurs because nuclear DNA encodes the majority of mitochondrial proteins and all the factors that regulate mtDNA replication and transcription (Castegna et al., 2015). It is well known the existence of a feedback of communication from mitochondria to nucleus, the "retrograde signalling", that influences many cellular functions under both normal and pathological conditions (Liu and Butow, 2006). Retrograde response results in changes in the expression of nuclear metabolic and stress genes and it is strictly related to autophagy and ageing (Jazwinski, 2013). The first

retrograde pathway identified was the RTG signalling. It depends on three cytosolic proteins: Rtg1, Rtg2, and Rtg3. Rtg2 is the activator of the pathway that allows the translocation of Rtg1 and Rtg3 from cytosol to nucleus. Rtg1 and Rtg3 are transcription factors that control the expression of genes coding for mitochondrial proteins (da Cunha et al., 2015). The activator of retrograde response, Rtg2, is a component of SILK, the SAGA-like complex containing also Gcn5 (Pray-Grant et al., 2002). It was shown that deletion of GCN5 causes an attenuation of the retrograde response similarly to deletion of RTG2 (Kim et al., 2004). The activation of stress response genes by Gcn5 is counteracting by corepressor complexes containing Rpd3 or Hda1 (Huisinga and Pugh, 2004). Interestingly, deletion of RPD3 or HDA1 has opposite effect compared to RTG2 deletion (Kim et al., 1999). Yeast offers a unique possibility to study nuclear or mitochondrial mutants exhibiting complete or very severe respiratory deficiencies and that can be easily recognized by defective growth on glycerol containing medium. Functional studies can be performed growing the cells by fermentative metabolism on glucose. Most of the knowledge about mitochondrial function and dysfunction comes from budding yeast. Mutants bearing equivalent human pathological substitutions have been constructed taken advantage of the similarity between human and yeast mitochondrial DNA and the possibility of transforming yeast mitochondria (Montanari et al., 2008). For all these reasons, in my PhD project we have studied the role of SAGA complex in respiration and in mitochondrial functions using yeast *Saccharomyces cerevisiae* as model system.

Aim of the work

Many efforts have been made to study the link between epigenetic and mitochondrial dynamics, but to date only few pathways have been well understood. The main aim of my research was to bring new knowledge about the epigenetic mechanisms that control nucleus-mitochondria communication and mitochondria functionality using yeast as model system. Preliminary results obtained in my group showed that the integrity of chromatin modifier SAGA complex was required for growth in respiratory condition. In my doctoral project, I have studied the role of SAGA in respiration and the possible involvement of KAT Gcn5 and DUB Ubp8 in mitochondria activity.

Results

SAGA complex and its catalytic activities are required in yeast respiration.

SAGA is a multi-protein complex with distinct catalytic and structural domains. In order to analyse the role of SAGA in *S. cerevisiae* respiration we tested the growth capability of strains deleted in subunits of the complex in three metabolic conditions. Serial dilutions of WT and strains deleted in genes of KAT Gcn5, DUB Ubp8, the Ubp8 assembly factor Sgf73 and the structural subunit Spt7 were spotted on solid media containing glucose 2% as fermentable carbon source, glycerol 3% as respiratory one or low glucose that allows both respiration and fermentation (Fig. 1A). Strain lacking GCN5 showed slow growth in all metabolic conditions and this defect was more evident in glycerol containing medium. Interestingly, strains deleted in ubiquitin protease Ubp8 and in structural subunit Spt7, needed for the integrity of the complex, showed the stronger defective phenotypes in respiratory condition compare to WT. These results suggest a role of SAGA complex and its catalytic modules in respiration. We next tested oxygen consumption capability of the above strains to confirm the involvement of SAGA in respiratory activity. As shown in Fig. 1B, strains *ubp8Δ* and *spt7Δ* were totally enable to consume oxygen, while *gcn5Δ* showed a slow ratio of consumption compared to WT (Canzonetta et al., 2016).
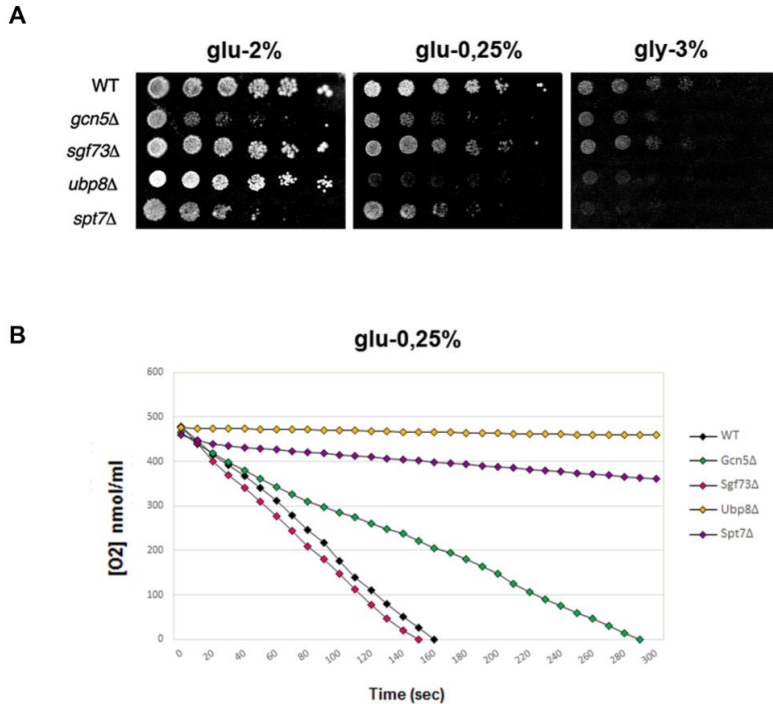
Fig. 1 Deletion of SAGA complex subunits results in defective respiration. A Serial dilutions of WT (W303-1A), *gcn5Δ*, *sgf73Δ*, *ubp8Δ*, *spt7Δ* strains grown in YP 2%, 0.25% glucose and 3% glycerol at 28 °C for 48 h. **B** Oxygen consumption rate of WT (black), *gcn5Δ* (green) *sgf73Δ* (red) *ubp8Δ* (yellow) *spt7Δ* (purple) cells grown in YP 0.25% glucose and collected at exponential phase.

Expression levels of Gcn5 and Ubp8 increase in respiratory condition.

Since SAGA catalytic subunits Ubp8 and Gcn5 are required for growth in respiratory medium and for oxygen consumption, we asked whether their expression could be differently regulated in

fermentation and respiration. qRT-PCR analysis of WT strain grown in glucose 2% or glycerol 3% containing media showed that GCN5 transcription was enhanced in respiration (Fig. 2A).
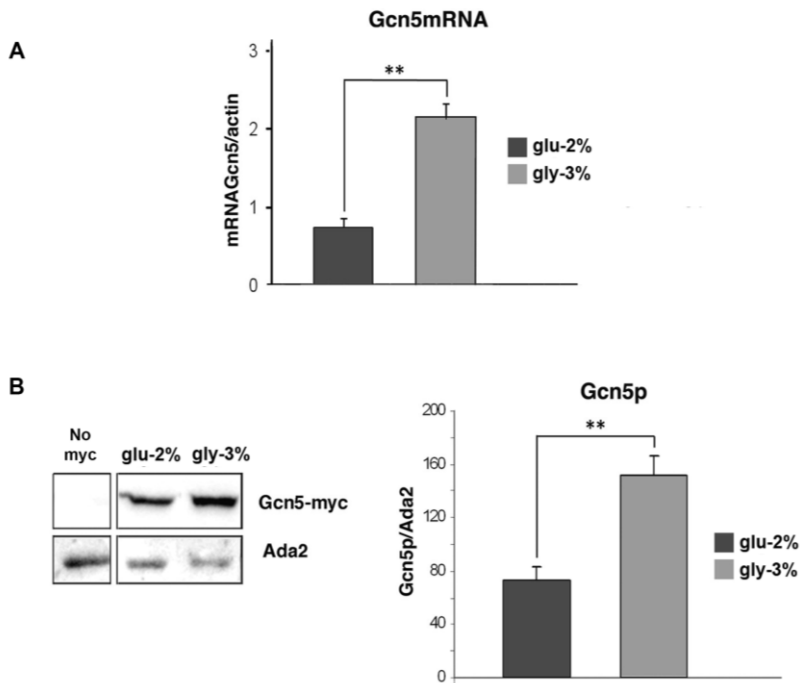
Fig. 2 Gcn5 expression is upregulated in respiratory condition. A qRT-PCR analysis of Gcn5 mRNA expression in a WT (W303-1A) strain grown in YP glu-2% (black) and YP gly-3% (grey), actin is used as housekeeping control. **B** Western blot analysis from total extracts of Gcn5-myc protein expression in WT strain grown in YP glu-2% and YP gly-3%, untagged control strain (No-myc) is shown. Histogram of Gcn5-myc protein expression in YP glu-2% (black) and YP gly-3% (grey) normalized to Ada2 loading control. Data are represented as mean + SEM. ** p value < 0,01.

To measure Gcn5 protein levels, we performed western blot analysis using a WT (W303-1A) strain carrying an integrated and functional tagged version of Gcn5 (Gcn5-myc). Total protein extracts from cells grown in YP glucose 2% or glycerol 3% were analysed on SDS-PAGE and western blot filter hybridized with anti-myc antibody. The Gcn5-myc signal was normalized to constitutive Ada2 using anti-Ada2 antibody (Fig. 2B). Results showed a significant increase of the protein in respiration, highlighting the needed of Gcn5 in this metabolic condition. Acetylation is closely linked to the metabolic state of the cell, so we decided to test the effect of HAT inhibitor CPTH2 (Chimenti et al., 2009) on Gcn5 protein expression levels. As shown in Fig. 3, treatment with CPTH2 500 μM for 4 and 7 h decreased Gcn5 levels with a reduction of 50% compared to solvent DMSO in both glucose and glycerol containing media.

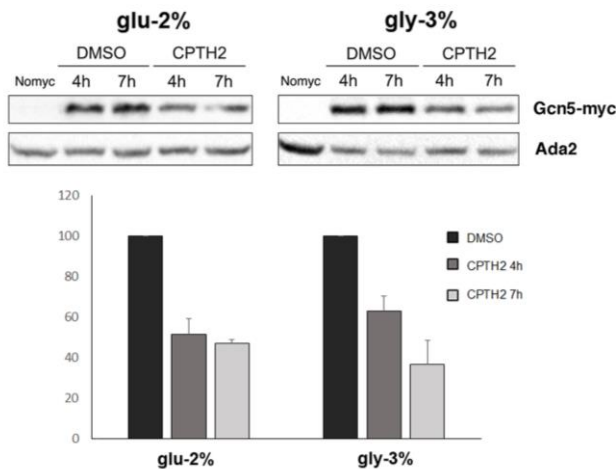**Fig. 3 Gcn5 expression strongly decreases after treatment with HAT inhibitor CPTH2.** Western Blot analysis of expressed levels of Gcn5-myc in WT strain grown in DMSO and CPTH2 (500 μM) for 4 and 7 h hybridized with anti-myc and anti-Ada2 control, untagged strain (No-myc) is also shown. Bands corresponding to Gcn5-myc were normalized to Ada2 and relative values are indicated respect to DMSO samples.

Similar experimental approaches were used to analyse Ubp8 regulation. As shown in Fig 4A and 4B, Ubp8 transcriptional and protein levels increased in respiratory condition similarly to Gcn5.
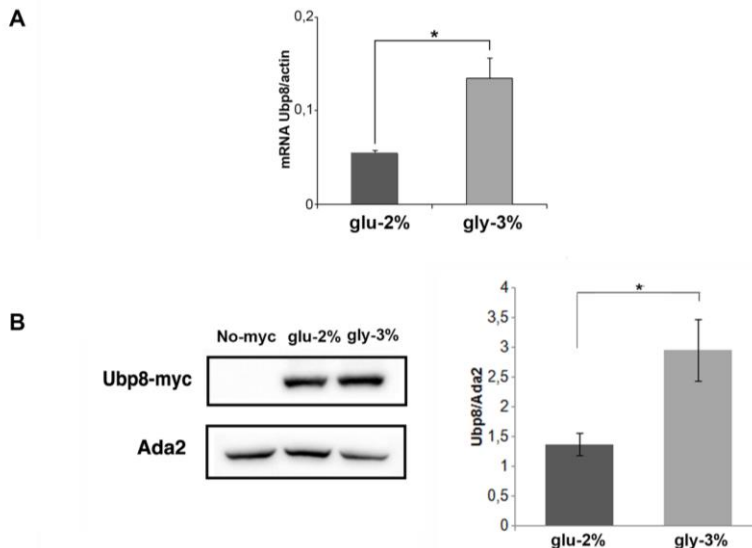

Fig. 4 Ubp8 expression is enhanced in respiratory condition. A qRT-PCR analysis of Ubp8 mRNA expression in a WT strain grown in YP glu-2% (black) and gly-3% (grey) normalized to actin as housekeeping control. **B** Western blot analysis from total extracts of Ubp8-myc protein expression in WT strain grown in YP glu-2% and YP gly-3%, untagged control strain (No-myc) is shown. Histogram of Ubp8-myc expression in glu-2% (black) and gly-3% (grey) normalized to Ada2 loading control. Data are represented as mean + SEM. * p value < 0,05.

On the contrary, CPTH2 treatment had no effect on Ubp8 protein level in glucose 2%, while in glycerol 3% the HAT inhibitor caused a strong decrease of protein expression (Fig. 5) (Leo et al., 2018). Collectively our results showed that Gcn5 and Ubp8 are upregulated

in respiratory medium at both transcriptional and protein levels. Interestingly, we found that Ubp8 expression is strongly influenced by acetylation specifically in respiratory condition.
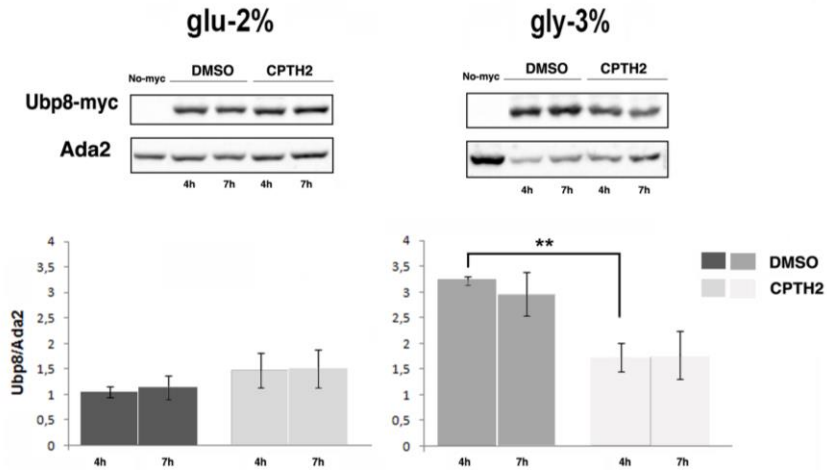
Fig. 5 Ubp8 expression is sensitive to CPTH2 in respiratory condition. Expression of Ubp8-myc and Western Blot analysis of total protein extracts of WT Ubp8-myc strain grown overnight in YP glu-2% and gly-3% and then incubated in DMSO and CPTH2 (500μM) for 4 and 7 h hybridized with indicated antibodies. Untagged strain (No-myc) is shown as control. Histogram shows the expression levels of Ubp8-myc normalized to Ada2. Data are represented as mean ± SEM. ** p value < 0,01.

Deletion of deacetylase Hda1 rescues the defective phenotype of *gcn5Δ* strain.

In order to highlight the pathway related to Gcn5 in respiration, we searched for a possible interactor of this KAT using a functional-genetic approach. Hda1 is a histone deacetylase known to have an opposing activity on histone acetylation compared to Gcn5 (Vogelauer et al., 2000). Moreover, deletion of HDA1 increased lifespan, contrary to phenotype of GCN5 deleted strain (Kim et al., 1999). To study the possible interplay between these chromatin modifiers we isolated the single and double deleted strains in HDA1 and GNC5. Serial dilutions of WT, *gcn5Δ, hda1Δ* and double deleted strains were spotted on YP glucose 2%, 0.25% and glycerol 3% plates (Fig. 6A). *hda1Δ* strain did not show growth defects compare to WT whereas deletion of HDA1 in *gcn5Δ* strain completely rescued the respiratory defect of single deleted strain. As previously shown, CPTH2 decreases growth capability of *gcn5Δ* strain (Chimenti et al., 2009). We tested the effects of the inhibitor on the above strains in the three metabolic conditions. Fig. 6B shows that CPTH2 500 μM inhibited the growth of single deleted strains in all media, but the higher inhibition was obtained in glycerol 3% containing medium, in which also the WT strain showed a sick phenotype. Interestingly, the double deleted strain *hda1Δgcn5Δ* was unaffected by CPTH2, also in respiratory condition. These results suggested that Hda1 is a functional interactor of Gcn5 in respiration. CPTH2 has a stronger effect in respiratory condition and the pathway in which the inhibitor acts is missing when both genes HDA1 and GCN5 are deleted. These data has been confirmed by oxygen consumption measurement (Fig. 6C). The CPTH2 treatment impaired oxygen consumption of the *gcn5Δ* strain, while the rate of consumption was restored in the double deleted strain *hda1Δgcn5Δ*.
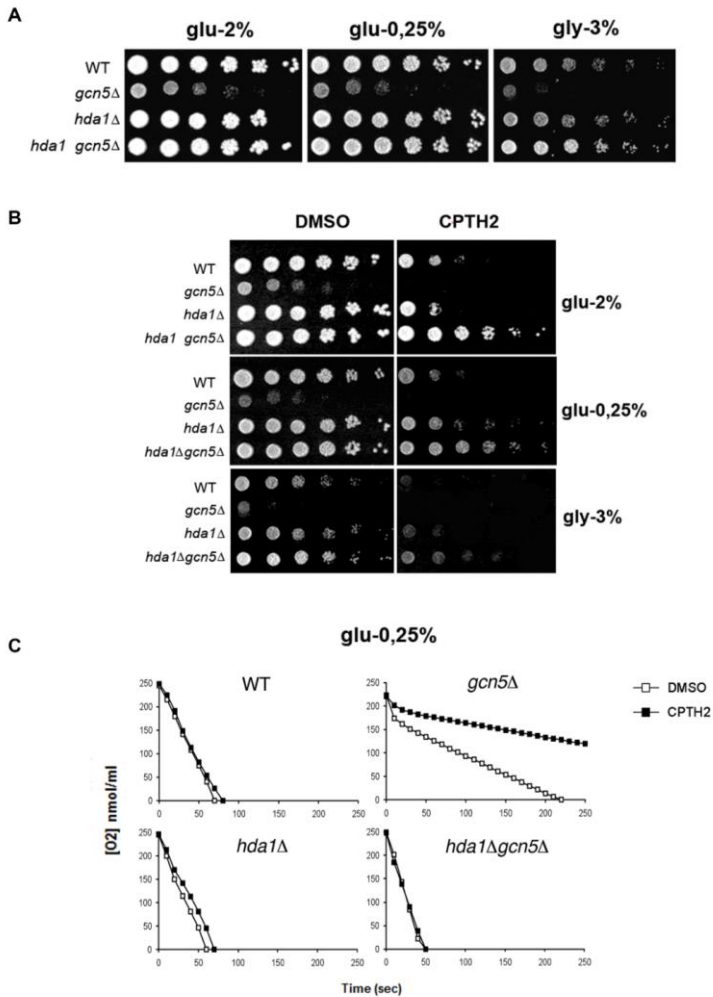
Fig. 6 Deletion of HDA1 rescues the defective respiration of *gcn5Δ* strain. A Serial dilutions of WT (W303-1A), *gcn5Δ*, *hda1Δ* and double *gcn5Δ/hda1Δ* strains were spotted on YP glu-2%, glu-0.25% and gly-3% plates and incubated at 28 °C for 48 h. **B** Growth spot assay of strains on YP glu-2%, glu-0.25% and YP gly-3% plates in the presence of solvent (DMSO) or CPTH2 (500 μM) incubated at 28 °C for 48 h. **C** Oxygen consumption rates (O_2 nmol/ml) of indicated strains grown in 0.25% glucose was measured after DMSO (open squares) and CPTH2 500 μM (filled squares) treatment for 4 h.

Gcn5 and Hda1 have opposite role on H3K18 acetylation.

It was shown that Gcn5 acts on histone H3 acetylation with a preferential activity on lysine K18 (Peng et al., 2008). Conversely, Hda1 has a role in histone H3 deacetylation (Yang and Seto, 2008). These findings prompted us to study changes in histones acetylation with the purpose to identify the common target of these chromatin modifiers. We performed western blot analysis of protein extracts from WT, *hda1Δ*, *gcn5Δ* and *hda1Δgcn5Δ* strains. Filter was hybridized with H3AcK18, H3AcK14, AcH3, unmodified UMH3 and Ada2 loading control antibodies (Fig. 7, left panel). The right panel shows the comparison with filter hybridized with AcH4, unmodified UMH4 and Ada2. In strain *gcn5Δ* acetylation of histone H3 was generally less compared to WT with a strong decrease in H3K18 residue. On the contrary, in *hda1Δ* strain we found an evident hyper-acetylation of lysine 18 of histone H3. These findings supported the idea that H3K18 is a specific target of the two enzymes.
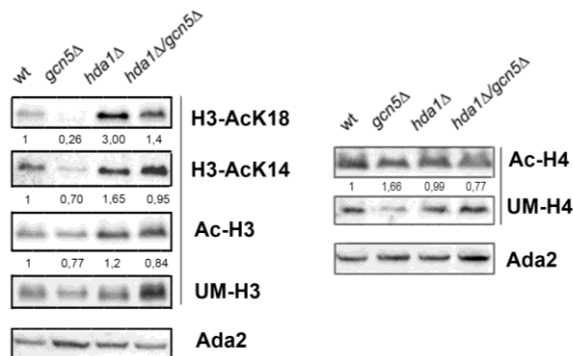
Fig. 7 Histone H3AcK18 is the preferential histone target for both Gcn5 and Had1. Western blot analysis of histones extracted from WT (W303-1A), *gcn5Δ*, *hda1Δ* and *hda1Δ/gcn5Δ* strains. Left panel, filter was sequentially hybridized with indicated antibodies H3AcK18, H3AcK14, AcH3 and normalized with UMH3. Right panel, AcH4 was normalized to UMH4. Indicated values represent the signal of each band normalized to the respective wild type level.

Next, we analysed histone H3 and H4 acetylation in protein extract from WT strain grown in glucose 2% or glycerol 3% containing media and treated for 7 h with CPTH2 500 μM and solvent DMSO. Fig. 8 shows that acetylation of lysine 18 was strongly affected by CPTH2 treatment, in particular in respiratory condition, while there was no effect on histone H4 acetylation and only a mild lowering of histone H3 total acetylation. Summarizing, H3K18 is a specific target of chromatin modifiers KAT Gcn5 and HDAC Hda1. Treatment with CPTH2 inhibits H3K18 acetylation and this effect is higher in respiratory condition.

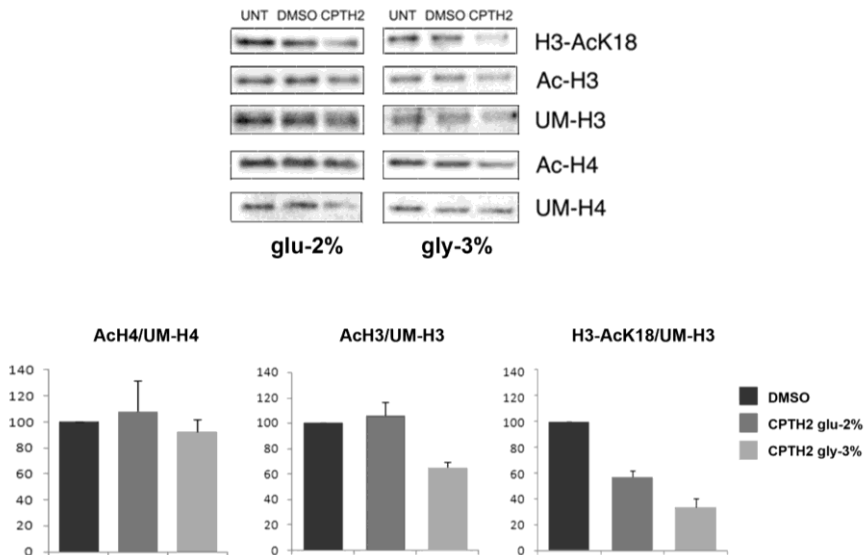**Fig. 8 CPTH2 treatment affects histone H3AcK18 acetylation.** Bulk histone preparation from WT cells grown in YP glu-2% or YP gly-3% and then treated with solvent DMSO and CPTH2 (500 μM) for 7 h. Filter was sequentially hybridized with indicated antibodies. Comparative histogram analysis showing the percentage of AcH4/UMH4, AcH3/UMH3 and H3AcK18/UMH3 normalized to solvent samples (DMSO as 100%).

Deletion of E3 Ubiquitin ligase Psh1 rescues the respiratory phenotype of *ubp8Δ* strain.

We observed the most defective respiration in the strain lacking DUB Ubp8 (Fig. 1). For this reason, we decided to study the interplay between ubiquitination and deubiquitination in metabolism. We tested functional genetic interactions of Ubp8 and two E3 ubiquitin ligases, Psh1 and Bre1, using single and double deleted strains. Serial dilutions of the strains were spotted on glucose 2%, 0.25% and glycerol 3% containing YP plates (Fig. 9A). As previously shown, strain deleted in UBP8 showed absence of growth in respiratory medium, while strains lacking the E3 ubiquitin ligases had a growth similar to WT cells in all tested conditions. Interestingly, in *ubp8Δ* strain the concomitant deletion of PSH1, but not the deletion of BRE1, totally rescued the defective phenotype caused by single deletion, suggesting an opposite role of Psh1 and Ubp8 in respiratory condition. We measured the O_2 consumption rate of the above strains, confirming a restoration of oxygen utilization in double deleted strain *ubp8Δpsh1Δ* (Fig. 9B). Next, we examined mitochondrial network with fluorescence microscopy using DASPMI staining of active mitochondrial membranes. As shown in Fig. 9C, Ubp8 deleted strain did not possess a tubular network with fluorescence diffused around vacuoles. Conversely, in *psh1Δ* and double deleted *ubp8Δpsh1Δ* strains mitochondria showed a WT network. These results showed that deletion of E3 Ub-ligase Psh1 totally suppresses respiratory defect of *ubp8Δ* strain suggesting that Psh1 acts on Ubp8 pathway with opposing effect.

A

B

C
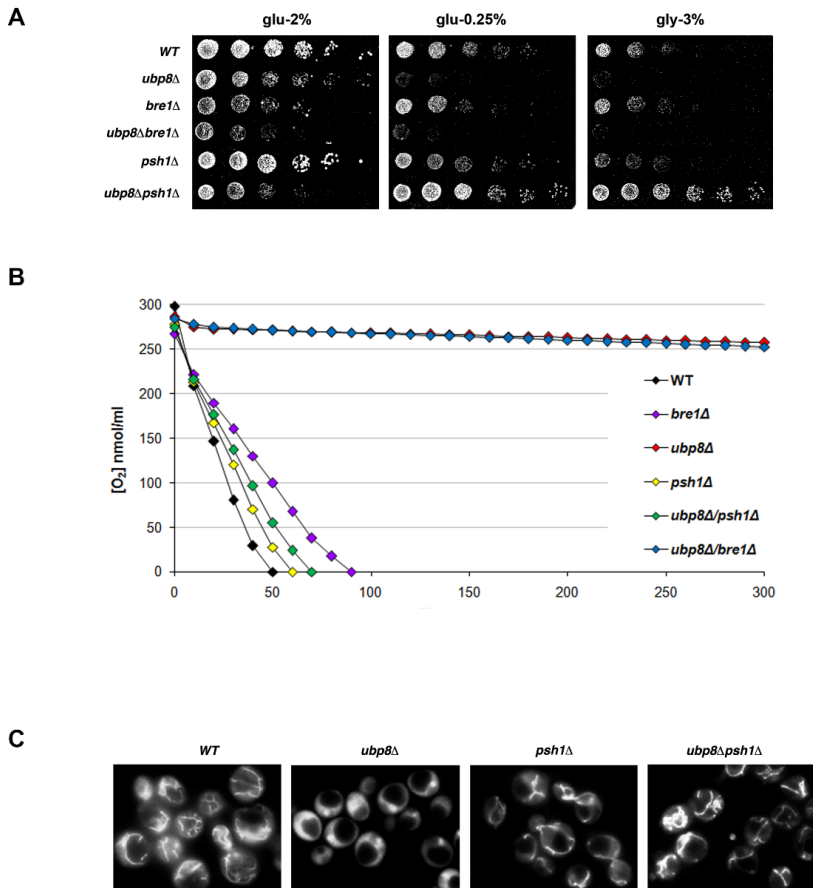
Fig. 9 Respiratory defects of *ubp8Δ* strain are rescued by deletion of E3 Ubiquitin-ligase Psh1. A Serial dilutions of indicated strains grown on YP glu-2%, 0.25 and gly-3% plates incubated at 28 °C for 48 h. **B** Oxygen consumption rate of WT (black), *bre1Δ* (purple), *ubp8Δ* (red), *psh1Δ* (yellow), *ubp8Δ/psh1Δ* (green) and *ubp8Δ/bre1Δ* (blue) strains. **C** DASPMI Fluorescence microscopy of WT, *ubp8Δ*, *psh1Δ*, *ubp8Δ/psh1Δ* strains.

Gcn5 and Ubp8 localize in mitochondria independently from SAGA complex.

HAT Gcn5 and DUB Ubp8 are known to localize in nucleus as chromatin modifiers. The defective respiratory phenotypes and the differential regulation of expression levels in fermentation and respiration let us wondered whether the proteins could localize in mitochondria. Mitochondria were purified from cells grown in YP glucose 2% or glycerol 3% containing media by differential centrifugations of whole cell lysate; proteins of both fractions were extracted and separated on SDS-PAGE. The analysis was performed using the tagged strains WT Ubp8-myc and WT Gcn5-myc and filter hybridized with anti-myc antibody. The quality of selective extraction was tested using antibodies against nuclear Ada2 and mitochondrial Por1 as controls. Results showed that Gcn5 and Ubp8 were present in nucleus/cytoplasm fraction, as expected, but they also localized in mitochondrial fraction (Fig. 10A and B). Moreover, Fig. 10A and B shows that expression level of Ubp8 in mitochondria was strongly upregulated in respiratory medium (gly-3%), while mitochondrial localization of Gcn5 was less influenced by carbon sources compared to N-C fraction. As shown in histogram of Fig 10B, the level of Ubp8 in mitochondria during respiration matched with a similar increase of the outer mitochondrial membrane porin Por1. This finding suggested an overall increase of mitochondrial mass in respiratory condition. Same figure shows that Ada2, subunit of SAGA HAT module, was present only in nucleus/cytoplasm fraction. This finding implies that Ubp8 and Gcn5 localize in mitochondria without SAGA complex. For this reason, we tested cell localization of Ubp8-myc and Gcn5-myc in strains deleted in SPT20, a structural subunit of SAGA needed for complex assembly (Fig. 11). Results showed that SAGA integrity is not needed for Ubp8 and Gcn5 mitochondrial localization. Moreover, in *spt20Δ* strain the amount of mitochondrial Ubp8 and Gcn5 was higher than in WT, suggesting that in absence of SAGA complex the two enzymes are free to be imported in mitochondria. Summarizing, we found that

Ubp8 and Gcn5 localize in mitochondria and that they could act in this cell compartment independently from SAGA complex.
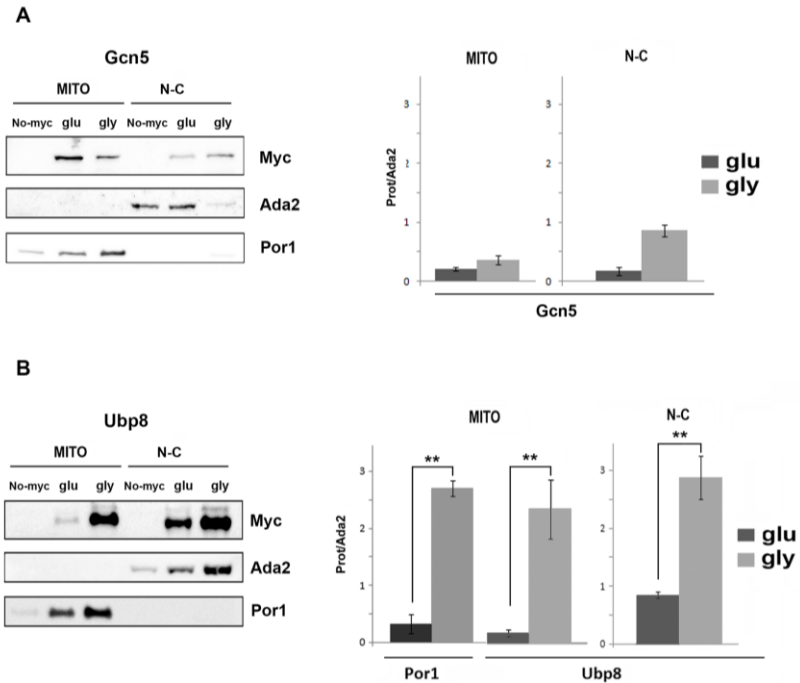
Fig. 10 Ubp8 and Gcn5 localize in both nucleus and mitochondrion. A Western Blot analysis of WT Gcn5-myc strain grown in YP glu-2% and gly-3% containing media and separated in mitochondrial (MITO) and nucleus-cytoplasmic (N-C) fractions, untagged control (No-myc) is shown. Filter was hybridized with anti-myc, anti-Ada2 for nuclear control and anti-Por1 for mitochondrial fraction. Histogram of Gcn5-myc and Por1 expression normalized to Ada2 loading control in the indicated samples and conditions is shown. **B** Subcellular fractionation and western blot of WT Ubp8-myc strain grown in YP glu-2% and gly-3%. Histogram of Ubp8-myc and Por1 expression normalized to Ada2 loading control in the indicated samples and conditions is shown. Data are represented as mean ± SEM. ** p value < 0,01.

Fig. 11 Disassembly of SAGA complex does not affect Ubp8 and Gcn5 mitochondria localization. Subcellular fractionation and western blot analysis of Gcn5-myc and Ubp8-myc in WT and *spt20Δ* strains.

E3-Ub ligase Psh1 localizes partially in mitochondria and its deletion affects Ubp8 localization.

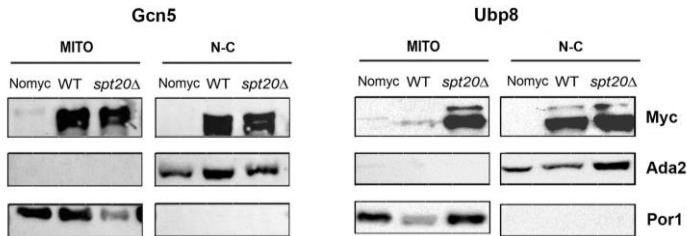Focusing on Ubp8 localization, we asked if also Psh1 could localize in mitochondria. Mitochondria were separated from nucleus/cytoplasm fraction in WT cells carrying a tagged version of Psh1 (Psh1-myc) after exponential growth in glucose 2% and glycerol 3% containing media. Fig. 12A shows that Psh1 localized in nucleus as expected, but it partially was found in mitochondrial fraction. This result suggested that Ubp8 and Psh1 could interact in ubiquitination/deubiquitination of mitochondrial proteins needed for an efficient mitochondrial activity. We then analysed the effect of PSH1 deletion in Ubp8 localization. We performed a cell fractionation in WT and *psh1Δ* Ubp8-myc strains grown in glucose 2% or glycerol 3% containing media (Fig. 12B and C). As shown in histograms, we found that in absence of Psh1 the amount of mitochondrial Ubp8 decreased in respiratory condition, while increases in fermentation. These finding suggest that Psh1 influences cell localization of Ubp8, reinforcing the idea of the interplay between these two epigenetic factors in mitochondria.
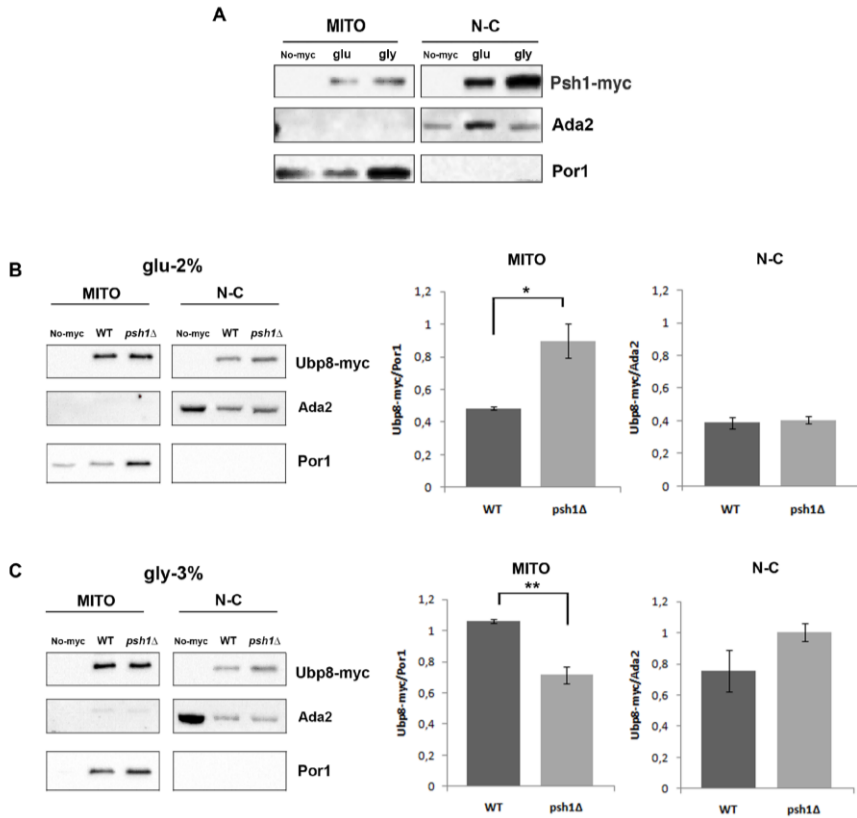
Fig. 12 E3-Ub ligase Psh1 localizes in mitochondria and its deletion affects the amount of mitochondrial Ubp8. A Western Blot analysis of Psh1 localization in WT Psh1-myc strain grown in YP glu-2% and gly-3% and separated in mitochondrial (MITO) and nucleus-cytoplasmic (N-C) fractions, untagged control (No-myc) is shown. Filter was hybridized with anti-myc, anti-Ada2 and anti-Por1 antibodies. **B** Subcellular fractionation and western blot of WT and *psh1Δ* Ubp8-myc strains grown in YP glu-2%. Histogram of Ubp8-myc expression level normalized to Por1 (MITO) and Ada2 (N-C) loading controls. **C** Subcellular fractionation and western blot of WT and *psh1Δ* Ubp8-myc strains grown in YP gly-3%. Histogram of Ubp8-myc expression level normalized to Por1 (MITO) and Ada2 (N-C) loading controls. Data are represented as mean ± SEM. ** p value < 0,01. * p value < 0,05.

Gcn5 is needed for Ubp8 expression and localization.

Next, we analysed the effect of Gcn5 and acetylation on Ubp8 expression and localization. Ubp8 mRNA expression was measured by qRT-PCR in WT and *gcn5Δ* cells grown in respiratory condition (gly 3%). Result showed a strong decrease of Ubp8 mRNA in strain lacking Gcn5 with respect to actin mRNA (Fig. 13A). Using cell fractionation, we compared the Ubp8 localization in WT and *gcn5Δ* strains after growth in glycerol 3% containing medium. Fig. 13B shows that in *gcn5Δ* strain the Ubp8 level was lower compared to WT cells in both nuclear and mitochondrial fractions. These results suggest that Gcn5 is implicated in regulation of Ubp8 transcription with effect on protein availability also in mitochondria compartment. Due to the inhibitory effect of HAT inhibitor CPTH2 on Ubp8 expression level in respiration (Fig. 5), we asked whether CPTH2 affects also mitochondrial Ubp8. We tested the effect of the drug in a mild respiratory condition to avoid any cell and mitochondria stress. WT Ubp8-myc cells were grown overnight in glucose 0.25% containing medium and then treated for 15 h with CPTH2 500 μM and solvent DMSO. Mitochondria were separated from nucleus/cytoplasm and analysed by western blot. As shown in Fig. 13C, Ubp8 expression decreased after treatment with CPTH2 compared to mitochondrial Por1. In conclusion, results showed a general requirement of acetylation for Ubp8 expression and for its normal cellular localization.

A

B

C
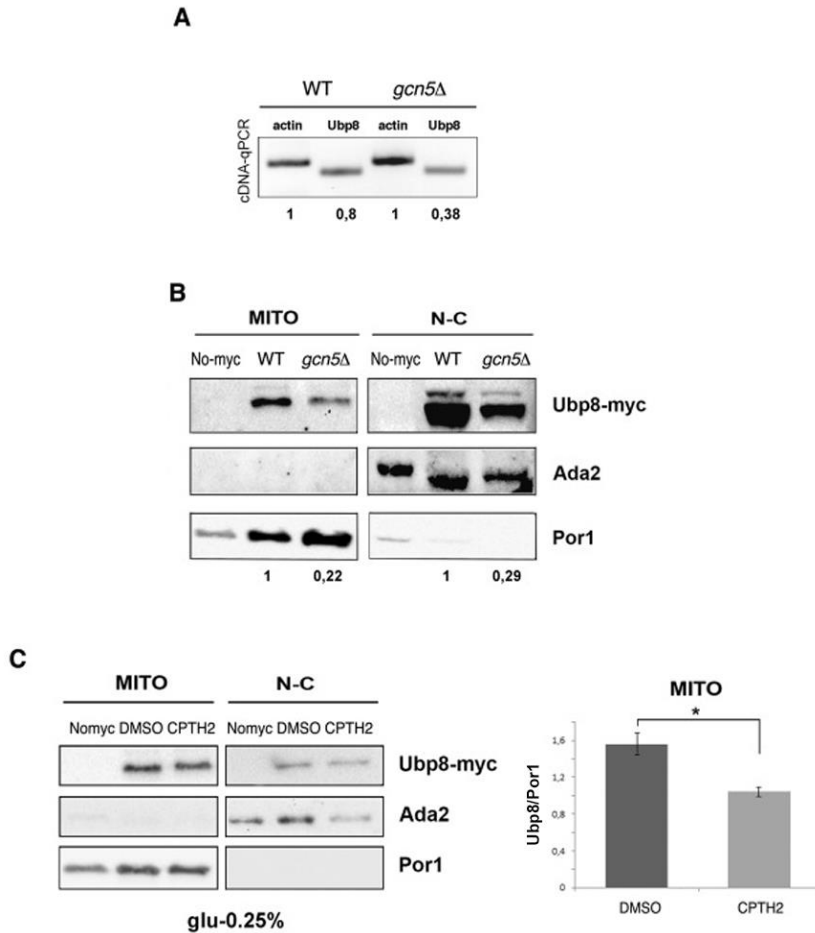
Fig. 13 Gcn5 regulates Ubp8 expression levels influencing its localization. A qRT-PCR analysis of Ubp8 mRNA expression in WT and *gcn5Δ* strains grown in YP gly-3% containing media, normalized to actin as housekeeping control. **B** Cellular fractionation and western blot of WT and *gcn5Δ* Ubp8-myc strains grown in YP gly-3%. Values of mitochondrial Ubp8/Por1 and nuclear Ubp8/Ada2 are shown. **C** Western blot analysis of cellular fractionation in WT Ubp8-myc grown in YP glu-0.25% and treated for 15h with CPTH2 500 μM or solvent DMSO at same final concentration. Histogram shows relative amount of mitochondrial Ubp8 normalised with Por1 intensities. Data are represented as mean ± SEM. * p value < 0,05.

Acetylation is specifically required for growth in respiratory condition.

To better characterize the interplay between acetylation and respiration, we compared the expression level of Ubp8 and Por1 after treatment with CPTH2 or Antimycin A, an inhibitor of respiratory chain complex III. WT Ubp8-myc cells were exponentially grown overnight in YP glycerol 3% containing media and then treated for 5 h with CPTH2 500 µM or Antimycin A 2µM. Total proteins were extracted and analysed by western blot. As shown in Fig. 14A and B, Ubp8 protein level decreased after treatment with CPTH2, while there was only a weak reduction of mitochondrial Por1 expression. Treatment with Antimycin A did not affect Por1 expression, while Ubp8 level was more sensitive to the inhibition of respiration. Interestingly, these data suggested that Ubp8 expression level changes in response to both cell respiration impairment and acetylation activity. Next, we compared the effect of CPTH2 and Antimycin A on growth of WT and isogenic deleted strains *ubp8Δ*, *psh1Δ*, *ubp8Δpsh1Δ*. Serial dilutions of the above strains were grown in YP glucose 2% or 0.25% solid plates with addition of CPTH2/DMSO or Antimycin A/EtOH. As shown in Fig. 14C, Antimycin A affected growth only in glu 0.25% containing media, while CPTH2 impaired the growth in both metabolic condition. In respiratory medium, the effect of CPTH2 was more evident, since *ubp8Δpsh1Δ* strain showed a severe growth defect. This finding reinforces the idea that acetylation is necessary in the pathway related to Ubp8/Psh1 in respiration.
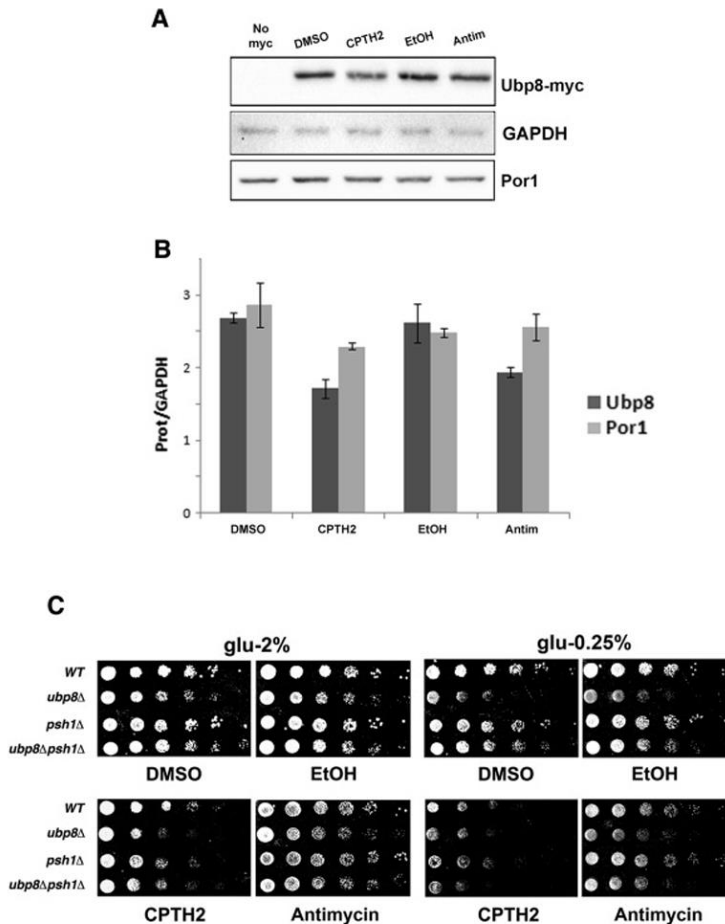
Fig. 14 Acetylation is necessary for efficient growth in respiratory condition. A Western blot analysis of Ubp8 and Por1 expression levels in WT Ubp8-myc grown in YP gly-3% and then treated for 5h with CPTH2 500 μM or solvents DMSO and Antimycin A 2 μM or solvent EtOH. **B** Histogram of Ubp8 and Por1 intensities normalised to GAPDH loading control. **C** Growth spot assay of WT, *ubp8Δ*, *psh1Δ*, *ubp8Δpsh1Δ* strains on YP glu-2% and glu-0.25% containing media in the presence of CPTH2 500 μM / DMSO or Antimycin A 2 μM / EtOH incubated at 28 °C for 48 h.

Discussion

In my doctoral thesis, we studied the role of SAGA complex in yeast respiration and we showed that the complex is necessary for respiratory activity. Focusing on its catalytic subunits, we found that HAT Gcn5 and DUB Ubp8 are required for respiration and, most importantly, we showed for the first time that they localize in both nucleus and mitochondria, underling a new function as mitochondrial factors. The finding that nuclear epigenetic factors can localize also in mitochondria reinforces the idea of their specific involvement in communication between nucleus and mitochondria, needed for efficient environmental response and cell behaviour regulation. It is known that nucleus controls mitochondrial functions through the 'anterograde response' that regulates mitochondrial activity and biogenesis. Conversely, mitochondria influence the expression of nuclear genes through the 'retrograde response' under stress condition and environmental changes (Matilainen et al., 2017). Moreover, mitochondrial metabolism controls levels of key molecules such as acetyl-CoA, intermediate of histone and non-histone protein acetylation. Acetyl-CoA is a sensor of energy status (Shi and Tu, 2015). When energy production is high, acetyl-CoA is available for histone acetylation, promoting gene transcription. In presence low energy production, acetyl-CoA level decreases with a reduction of histone acetylation and consequent chromatin condensation (Menzies et al., 2016). We studied the role of SAGA using cellular and molecular approaches. Results shown in Fig. 1 demonstrated a direct role of SAGA complex and the requirement of its catalytic activities in regulation of respiratory capability. We found that Gcn5 and Ubp8 are upregulated in respiration at both transcriptional and protein levels. Moreover, we tested the effect of HAT inhibitor CPTH2 on Gcn5 protein, finding a reduction in both fermentation and respiration. Interestingly, CPTH2 had no effect on Ubp8 expression levels in cells grown in glucose containing medium, but it was able to decrease the protein level when cells were grown in glycerol containing medium (Fig. 3), suggesting a specific role of

acetylation in regulation of Ubp8 in respiration. These results point out the existence of a modulation of Gcn5 and Ubp8 expression dependent on metabolic state of the cell and related to acetylation activity. The switch between fermentation and respiration is known to cause a wide reprogramming of gene expression. The master regulator of non-fermentative metabolism is Snf1, serine/threonine protein kinase homologue of human AMPK. Interestingly, it has been shown that Ubp8 directly regulate Snf1 stability and activation via protein deubiquitination (Wilson et al., 2011). On the other hand, Snf1 regulates Gcn5 occupancy and cooperates with it at promoter regions of metabolic genes (Liu et al., 2010, Abate et al., 2012). Further studies will be needed to understand whether the modulation of Gcn5 and Ubp8 expression occurs upstream Snf1 activation or whether it could be a feedback regulation with consequent signal amplification. The data that deletion of Gcn5 lowers Ubp8 expression at transcriptional level suggests that Gcn5 acts upstream Ubp8 promoting its gene expression. To analyse the pathway of Gcn5 and Ubp8 in respiration, we used a functional-genetic approach. As shown in Fig. 6, the defective phenotype of *ubp8Δ* strain in respiratory condition was rescued by the deletion of E3 ubiquitin ligase Psh1. This enzyme is involved in ubiquitination of centromeric histone Cse4 and cooperate with Ubp8 to regulate its localization at centromere (Canzonetta et al., 2015). Analysis of mitochondria morphology and growth phenotype of single and double delete strains in genes UBP8 and PSH1 in respiratory condition suggest the existence of a common target different from Cse4 not yet identify. Deletion of histone deacetylase HDA1 was able to recover defective phenotype of strain *gcn5Δ* in respiratory condition confirming that Hda1 is an interactor of Gcn5. Hda1 is a subunit of histone deacetylase (HDA) complex that counteract SAGA activity (Carmen et al., 1996) having opposite function. It is interesting to note that HAT inhibitor CPTH2 appeared to have no effects on *gcn5Δhda1Δ* strain contrary to WT and that the acetylation level of the preferential target (lysine 18 of histone H3) decreased after CPTH2 treatment (Fig. 4 and 5). These results suggest a model in which Gcn5 and Hda1 have opposite role on histone H3K18 acetylation modulating gene transcription in response to carbon

source. Next, we wondered if Gcn5 and Ubp8 could act in other cell compartments beyond the nucleus. Surprising, results showed that they localize also with the mitochondria fraction. We demonstrated that mitochondrial localization of Gcn5 and Ubp8 is differently regulated in response to carbon source in growth medium. Moreover, we showed that Gcn5 and Ubp8 localize in mitochondria independently from SAGA complex, highlighting a possible mitochondrial activity as single proteins. Preliminary data showed that Ubp8 localize in protein fraction of outer mitochondria membrane and intermembrane space, while Gcn5 was found in the inner mitochondrial membrane (data not shown). These results may suggest two different and independent mitochondrial functions. Few years ago, mitochondrial protein acetylation was supposed to be consequence of non-enzymatic mechanisms due to chemical reactivity of lysine residues towards acetyl-CoA (Baeza et al., 2015). Later, it was found that human acetyltransferase MOF is enriched in mitochondria in which binds mtDNA and is essential for oxidative phosphorylation (Chatterjee et al., 2016). Gcn5L1, mammalian homologous of Gcn5, was found to localize in mitochondria (Scott et al., 2012) controlling levels of mitochondrial protein acetylation. Interestingly, it seems to be involved in mitochondrial autophagy (Scott et al., 2018). The finding that yeast Gcn5 is present in mitochondria highlights a possible conserved mechanism as regulator of mitochondria turnover and biogenesis. Moreover, the localization of Gcn5 in inner mitochondria membrane suggests that it could be involved in acetylation of mitochondrial cristae proteins or could interact with matrix components. Quality control of mitochondrial function is due to a specific pathway, named mitophagy, depending on Ubiquitin–Proteasome system (UPS). In mitophagy, the UPS-mediated degradation of damaged mitochondria prevents fusion with healthy mitochondria. The two master regulators of this mechanism are mitochondrial kinase PINK1 and cytosolic E3 ubiquitin ligase PARKIN (Jin et al., 2010, Jin and Youle, 2013). Less is known about degradation of intra-mitochondrial proteins. It has been shown that internal proteins are targets of ubiquitination and can be retro-translocated outside mitochondria, but it is unclear if addition of

ubiquitin molecules occurs inside mitochondria or in cytosol before import (Bragoszewski et al., 2015, Radke et al., 2008). A recent study suggests that the turnover of proteins implicated in oxidative phosphorylation is regulated inside mitochondria by ubiquitination in response to energy metabolism (Lavie et al., 2018). In human, only three DUBs, USP8, USP15 and USP30, show mitochondrial localization (Durcan and Fon, 2015). In yeast, only DUB Ubp16 was identify in outer mitochondrial membrane, but its function is unknown (Kinner and Kolling, 2003). The finding that Ubp8 localizes in mitochondria represents a new step in understanding the intricate and not yet understood mechanism of mitochondrial proteins regulation and turnover. Our results showed that also Psh1 localizes in nucleus and mitochondria suggesting a mitochondrial function opposite to Ubp8. In absence of Psh1, mitochondrial Ubp8 level decreases in respiratory condition while increases in fermentation (Fig. 8). This finding reinforces the idea of a close mitochondrial activity of Psh1 and Ubp8 during respiration with a possible role in targeting proteins to degradation. Moreover, results showed that Ubp8 and mitochondrial protein Por1 are influenced by acetylation state in respiratory condition demonstrating a general requirement of acetylation in mitochondrial activity (Fig. 10). One question remain to elucidate: how are these nuclear proteins imported in mitochondria? Until now, five different import mechanisms were identify, but evidences suggest the existence of other pathways not yet understood (Wiedemann and Pfanner, 2017). The majority of matrix proteins possesses a mitochondrial presequence that undergo cleavage after the import (Abe et al., 2000). Proteins without presequence possess different internal targeting signals or a particular hydrophobicity and are carried by small TIM chaperones (Sirrenberg et al., 1996). Although neither Ubp8 nor Psh1 possess an evident mitochondrial presequence, it is interesting to note that both of them show a possible recognition motif for TOM20, subunit of the main complex involved in translocation in mitochondria (Fukasawa et al., 2015). Moreover, Ubp8 was found to interact with two subunits of TIM complex, TIM 18 and TIM44 (Lee et al., 2011, Collins et al., 2007). On the contrary, the analysis of Gcn5 sequence does not show any presequence or recognition motif. This places Gcn5 in the

group of mitochondrial proteins for which the import pathway is still unknown. We could hypothesize a mechanism not related merely to the amino acids sequence. One possibility could be the involvement of protein post-translation modifications able to mimic a targeting signal or to alter the physical properties of the protein. Further studies are needed to test this hypothesis. Summarising, we found that SAGA and its catalytic modules are necessary in yeast respiration. In nucleus, Gcn5 counteract HDAC Hda1 in histone H3 acetylation and is needed for Ubp8 expression. Furthermore, we found that Gcn5 localizes in mitochondria with a possible role in mitochondrial protein acetylation and turnover. The absence of Ubp8 totally impairs respiration and abolishes mitochondria network. We found that deletion of Psh1 rescues mitochondrial defect of *ubp8Δ* strain highlighting an opposite activity respect to Ubp8. Surprising, both Ubp8 and Psh1 localize in mitochondria and the presence of Psh1 influences the localization of Ubp8, confirming a possible interplay in this organelle. To understand the mitochondrial role of Gcn5, Ubp8 and Psh1 will be necessary to identify mitochondrial targets and their possible post-translational regulation. Due to the sick phenotype of *ubp8Δ* in respiration, we can ask if it has a role in regulation of oxidative phosphorylation complexes or mtDNA inheritance. Moreover, we will be interesting in dissect the pathway related to mitophagy and mitochondrial proteins turnover in presence or absence of Gcn5 and Ubp8. Understanding the link between epigenetic and metabolism is crucial to identify mechanisms mis-regulated in disease. A wide range of diseases are associated to metabolic dysfunction, from neurodegenerative disorders to cancer. As clear example, mutations in gene of mitophagy activator PARKIN are associated to Parkinson syndrome (Dawson and Dawson, 2010). It is well known that many cancers are linked to Warburg effect that causes the establishment of anoxic metabolism (Liberti and Locasale, 2016). Interestingly, human orthologous of Ubp8, USP22, is a putative oncogene and is required for MYC-driven transcription (Zhang et al., 2008). Our work could improve the knowledge about the interplay between epigenetic and

metabolism with the perspective that the findings obtained in yeast could be helpful in understanding the complexity of human diseases.

Part II

Re-entrant DNA gels

Introduction

Nanoscience is the study of nanoscale materials and their application. Nanotechnologies are widespread in all scientific fields and are becoming part of the everyday life. The impact of nanotechnology in biology and medicine brought to the emergence of the nanobiotechnology, which is the study of biocompatible, non-toxic and efficient nano-based therapies and diagnostic techniques (Singer et al., 2018). Different kind of nanoparticle has been designed for medical purpose, such as liposomes and carbon nanotubes, but many of them cause toxicity and inflammatory reactions when injected in human body (Gharpure et al., 2015). In this scenario, the use of DNA as nanoscale material has attracted the interest of many scientists. DNA possesses unique properties, such as its biological function and the biocompatibility. Moreover, DNA shows physical characteristics that allow creation of secondary structures in a controlled manner. The concept of DNA material is based on the propriety of single strand DNA to anneal specifically with the complementary sequence following Watson and Crick base pairing and producing double strand molecules. This characteristic can be use to design synthetic DNA sequences able to anneal each other and create the desired secondary structures. DNA double strand can be flexible or rigid basing on the nucleotide sequence; more important, it can be denatured or re-annealed varying the temperature and allowing formation of reversible structures. Nadrian Seeman was the pioneer of DNA nanotechnology and in 1980s he started to evaluate the properties of DNA beyond its biological function (Seeman, 2003). Different DNA nanostructures were designed, including cubes (Chen and Seeman, 1991), polyhedral (Zhang and Seeman, 1994) and rings (Mao et al., 1997). The chemical and physical characteristics of DNA make it suitable for development of hydrogels, a class of colloids consisting in hydrophilic polymers immersed in solvent with both

solid and liquid properties (Wang et al., 2017). Due to the biocompatibility, many DNA hydrogels has been designed for drugs and proteins encapsulation and release in human body (Um et al., 2006, Shahbazi et al., 2018). I took part in a project born from the collaboration of Physic Department Sapienza University and IBPM Institute CNR. The aim of the work was the design of a DNA solution composed by long and short oligomers that shows a liquid state at high and low temperatures and able to spontaneously assembly in a gel at 37 °C. In brief, the DNA gel consisted of double strand tetramers able to bind each other to form a network. The propriety to liquefy at high temperatures reflects the melting of tetramers network. At low temperatures, the liquid state is caused by competition of short oligomers with tetramers that lead to the loss of the network (Fig 1A). The gel was designed using two types of DNA sequences: 57-bases oligomers and 6-bases competing oligomers. Four 57-bases oligomers were designed to be complementary to each other and form at high temperature a double strand tetramer with a flexible core. Moreover, sticky ends of 12 bases were designed for each arm of the tetramer in order to self-anneal and form tetramer-tetramer bond (bond A-A). Two 6-bases oligomers were created to be complementary to tetramer sticky ends (A-B bond) and to compete with A-A bond (Fig. 1B). The ability was to choose DNA sequences in which A-B were energetically stronger than the A-A bonds in order to be the relevant bonds at low T, but to work only at temperatures smaller than A-A bonds annealing. The gel formation was analysed by dynamic light scattering (DLS), a technique that allows to define the size distribution of small particles in solution. Results showed that cooling the system from 50 °C to 38 °C led to gel formation with the A-A as preferential bonds. At temperature lower than 25 °C, the bonds between sticky ends and 6-mers competitors became favourite and the A-B bonds replaced A-A gel. The dynamic light scattering results confirmed the theoretical prediction of "re-entrant" gel formation.
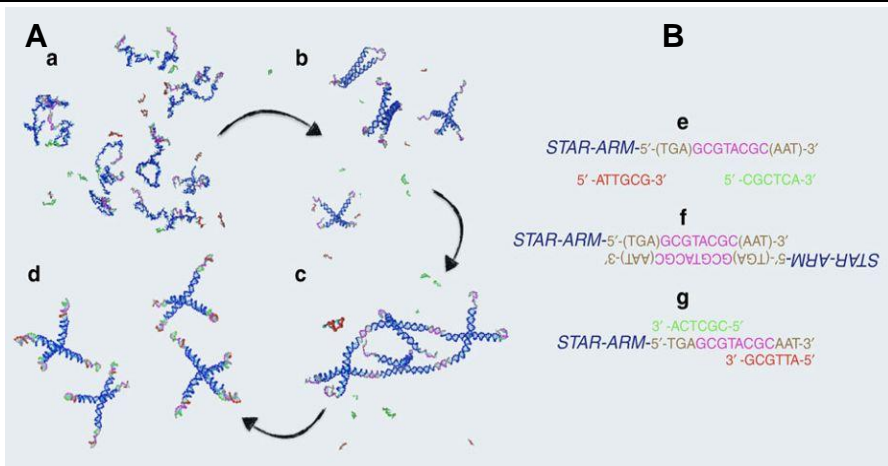
Fig. 1: Sketch of the DNA sequences and of their aggregation state. A Schematic representation of T dependant re-entrant gel formation: a) at very high temperature, neither tetramers nor competitors are able to anneal; b) cooling the system allows tetramers annealing; c) at intermediate temperature, tetramers sticky ends start to annealing each other with gel formation; d) low temperature let to competition between tetramers and 6-bases oligomers and the gel became less favourite. **B** Sequences composing the sticky ends (brown and pink) and 6-bases competitors (green and red).

Results

Gel formation and re-entrant phase measurement

Theoretically, when tetramers are annealed to each other, the number of sticky ends available for gel formation changes from four to zero based on temperature. This system can be compared to T-dependent colloid particles (A and B) characterized by separation in liquid and solid phases (Tlusty and Safran, 2000, Russo et al., 2011). In our case, it consists in the separation of tetramers from aqueous solution containing 6-bases oligomers. To verify the theoretical prediction, we decided to test experimentally the temperature dependent gel formation and phase separation. For DNA tetramers formation we

mixed equimolar quantities of the four 57-bases oligomers in a solution of NaCl 130 mM. We added the small 6-bases competitors to solution with a ratio of 4:1 in respect to tetramers in order to have no surplus of molecules. Samples were heated at 90 °C for 20 min and slowly cooled down to allow tetramers formation. We prepared samples at increasing concentrations (26, 39, 78, 100, 117 and 156 µM) and marked with ethidium bromide (EtBr) to detect double strand DNA. Samples were inserted in glass capillaries and centrifuged overnight at 4400 rpm at specific temperature to favour the establishment of a phase separation. To detect the presence and the position of the two phases, DNA was visualised using Chemidoc imaging system to detect EtBr signal. As shown in Fig. 2A, the homogeneous phase changed in response to tetramers concentration and temperature. At low concentrations, 26 and 39 µM, samples easily separated in two phases. Increasing concentration reduced the ability of separation and it was evident only in the range temperature of optimal gel formation (A-A bonds), as shown in samples 78 and 100 µM (Fig. 2A and B). At high concentrations, the density of tetramers prevented the separation of aqueous phase and the solution appeared homogeneous. It is interesting to note that at low temperature, when 6-bases competitors are bonded to tetramers (A-B bonds), the gel of A-A tetramers is not formed and the solution is homogeneous. The same phenomenon is observed at temperature higher than melting temperature of tetramers sticky ends, in which the formation of the gel was not allowed. These results confirm the goodness of the designed system, as shown in phase diagram of Fig. 2C.
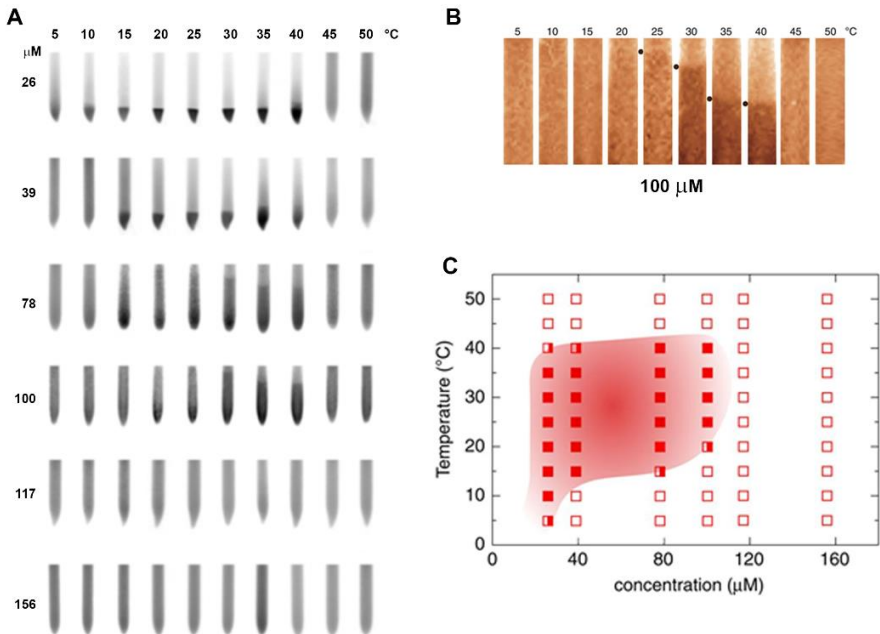
Fig. 2 Phase diagram of the re-entrant DNA gel. A Photographs of EtBr UV detection after overnight centrifugation at 4400 rpm at specific temperatures to enhance phase separation of samples prepared at different concentrations. Separation is visible as dark and light grey interface in sample from 26 to 100 µM. **B** Coloured photograph of the 100 µM sample at different T. Black points indicate the interface of phase separation. **C** Phase diagram of all concentrations and temperatures tested: filled squares indicate phase separated state points, open squares indicate stable homogeneous solutions and semi-filled squares indicate borderline cases.

Discussion

In the present work, we demonstrated the production of DNA material with the peculiar characteristics to self-assembly and to make a gel at specific temperatures. Authors theoretical designed a hydrogel with liquid proprieties at temperatures lower than 25 °C and higher than 50 °C, but able to assembly in gel at 37 °C, the human body temperature. We experimentally tested the theoretic prediction and the coexistence of a phase separation. We studied the system analysing EtBr intercalation in the double strand of DNA tetramers and found that gel formation occurs in the range of temperatures between 38 °C and 25 °C. Moreover, results showed that phase separation is dependent on samples concentration and is observed specifically in the temperatures range of gel formation. Our experimental analysing confirmed all theoretical predictions. The particular temperature dependent behaviour of the gel shows promising applications in nanobiotechnology. One of the main target of nanomedicine is the incorporation of bioactive molecules in nanoparticles to allow efficient cross of physiological barriers, controlled release of the drug and degradation within organism. Various DNA gels were designed for controlled drug delivery (Shahbazi et al., 2018). For example, a DNA hydrogel was developed for DOX and insulin release (Lee et al., 2012). Camptothecin also has been successfully encapsulated in DNA gels (Um et al., 2006). Interestingly, unmethylated CpG dinucleotides within DNA hydrogel were used as adjuvant for increase the immune response of ovalbumin, taking advantage of the propriety of these dinucleotides to stimulate Toll-like receptor (Nishikawa et al., 2014). The majority of DNA hydrogels designed for drug release are assembled by chemical or enzymatic reactions; the advantage of DNA system constructed by the authors of the present work is the spontaneous assembly propriety that allows, in principle, the gelation after injection in human body. The next aim of the study will be to test the ability of the gel to carry bioactive molecules in human cells in a controlled manner. The gelation after injection in a specific

organ should prevent the spread of molecules in non-target areas. Another possibility is the use of DNA gel to enhance the immune response against malignant cells. This should be possible designing DNA sequences with immunogenic bacterial motifs able to stimulate TLR9 and pro-inflammatory cytokines (Luis, 2008). In this scenario, the construction of a re-entrant self-assembly DNA gel represents a novelty for future therapeutic approaches.

EXPERIMENTAL MODEL AND SUBJECT DETAILS

Yeast strains used are Mating type A and listed in KEY RESOURCES TABLE. Yeast cells were grown at 28 °C under shacking in YP medium (1% yeast extract, 2% bactopeptone) containing 2%, 0.25% glucose or 3% glycerol. For drugs treatment, cells were grown overnight and drugs added to exponential cultures (0.3 OD_{600}/ml) for indicated times. Cyclopentylidene-[4-(4-chlorophenyl)thiazol-2-yl)hydrazine] (CPTH2) and Antimycin A were dissolved respectively in DMSO and EtOH and used at 500 μM and 2 μM final concentration. DMSO and EtOH were used at corresponding concentration as solvent control.

METHOD DETAILS

Yeast spot assay
For growth spot assay, 1 OD_{600}/ml of exponentially growing cells were serially diluted (1/5) and spotted on solid medium (2% agar). CPTH2 500 μM final concentration and DMSO were added directly on growth medium. Yeast cells were grown at 28°C for 48 h.

O2 consumption measurement
O2 consumption assay was performed using a Clark oxygen electrode Hansatech Instruments. 0.03 g (wet weight) of yeast cells were collected after growth in YP 0.25% glucose medium, washed with 1 ml sterile water and resuspended in 1 ml of 10 mM Na-phosphate buffer pH 7.4 containing 20 mM glucose. Samples were loaded in Reaction Vessel of a previously calibrated Oxygen Electrode Chamber.

Real time RT-PCR
For qRT-PCR experiments, cells of WT W303-1A or isogenic *gcn5Δ* strain were collected after overnight growth in YP containing 2% glucose or 3% glycerol as carbon source. Total RNA was extracted using phenol method and treated with DNAsi kit (Ambrion). cDNA was generated and 5 ng were analysed for each sample. Standard

curves were constructed using serial dilutions of WT DNA. Quantitative RT-PCR (qRT-PCR) experiments were carried out on a Rotor-gene Q (Qiagen) apparatus. All transcripts were measured at least in three independent experiments against ACT1 transcription level.

Total protein extraction, Western and Immunoblot
Yeast cultures grown at 28 °C under shaking in appropriate medium were collected at exponential phase (0.8 OD_{600}/ml). For drugs treatment, CPTH2 and/or Antimycin A were added to exponentially growing culture (0.3 OD_{600}/ml) and cells were harvest at various time as indicated in figure legends. Cell pellets were treated with 0.3 M NaOH, 140 mM βME, vortexed and incubated on ice. TCA 5.5% final concentration was added followed by further incubation on ice. After centrifugation, cells were lysed in HU buffer (8 M urea, 5% SDS, 200 mM Tris pH 6.8, 0.1 mM EDTA, 100 mM DTT, bromophenol blue) and boiled 15 min at 65 °C. Protein extracts were loaded on 10% SDS–PAGE, run and blotted on nitrocellulose membranes (Amersham). Western Blots were hybridized with primary antibodies listed in KEY RESOURCES TABLE. Proteins were detected by Long Lasting Chemilumiscent Substrate (EuroClone) and visualized by ChemiDoc™ MP Imaging System (Biorad). Signals were quantified by ImageLab analysis software.

Preparation of mitochondria
For mitochondria purification, yeast cultures were grown overnight at 28 °C under shaking and harvested at exponential phase (0.8 OD_{600}/ml). For each sample, 14 OD_{600} of cells were first treated with 10 mM DTT and 50 mM TrisHCl pH 9.5 for 15 min. Then, cells were incubated in spheroplast buffer (1.2 M sorbitol, 50 mM potassium phosphate pH 7.4, 1 mM MgCl, 250 μg of zymolyase per ml) for 1 h at 30°C. Spheroplasts were harvested by centrifugation for 5 min at 5000 rpm, washed with 1.2 M sorbitol and then lysed mechanically with Lysis buffer (600 mM sorbitol, 10 mM TrisHCl pH 7.4, protease inhibitor cocktail Roche) plus 0.8 g glass beads. Samples were serially centrifuged at 2500 rpm to remove unbroken

cells and debris. Mitochondria were separated from supernatant containing nuclear and cytoplasmic proteins by spinning down at 13000 rpm for 15 min and washed twice with Lysis buffer. For nuclear/cytosolic protein precipitation, TCA was added at 5.5 % final concentration, incubated 30 min at 4°C and centrifuged 15 min at 13000 rpm. Finally, mitochondria and nuclear/cytosolic samples were resuspended respectively in 20 μl and 50 μl of Laemmli buffer 2X (125 mM TrisHCl pH 6.8, 4% SDS, 20% glycerol, 285 mM β-mercaptoethanol, 2% bromophenol blue), boiled 10 min at 95°C and loaded on PAGE. After signal detection, proteins were quantified considering the volume loaded for each sample.

Fluorescent imaging
For microscopy analysis active mitochondria membranes were detected adding 1:1 DASPMI [2-(4-(dimethylamino)steryl)-1-methylpyridinium iodide] vital stain at a final concentration of 100 μM to an exponential growing culture on a glass slide and immediately visualized by fluorescence microscopy on Zeiss Axio Imager Z1 Fluorescence Microscope. Images were acquired by Axio-Vision 4.8 Digital Image Processing System and objective lens 63x oil.

QUANTIFICATION AND STATISTICAL ANALYSIS

Each experiment represents the average of at least three different biological replicates. Western blots were analysing using Image Lab software (Biorad). qRT-PCR were analysing using Rotor-Gene Q series software. Statistical analysis were performed using Microsoft Excel. Means and Standard errors are shown in figures. Asterisks represent significance and are as follows: ** $p < 0.01$, * < 0.05. Statistical analysis was performed with the Student's t-test.

KEY RESOURCES TABLE

REAGENT or RESOURCE	SOURCE	IDENTIFIER
Antibodies		
c-myc	Santa-Cruz	sc-40
ADA2	Santa-Cruz	sc-6551
Porin	Invitrogen	459500
H3	Abcam	ab1791
Acetyl H3	Millipore	06-599
Acetyl H3 (K14)	Abcam	ab52946
Acetyl H3 (K18)	Abcam	ab1191
H4	Millipore	N/A
Acetyl H4	Millipore	06-866
Chemicals, Peptides, and Recombinant Proteins		
Cyclopentylidene-[4-(4-chlorophenyl)thiazol-2-yl)hydrazine]	Prof. Antonello Mai	N/A
Antimycin A	Sigma	A86740
Experimental Models: Yeast Strains		
W303-1A WT *MATa ade2–1 trp1–1 leu2–3112 his3–11,15 ura3 can1–100 ssd*	(Vernarecci et al., 2008)	N/A

***ubp8Δ** MATa ade2–1 trp1–1 leu2–3112 his3– 11,15 ura3 can1–100 ssd. ubp8::His3MX6*	(Canzonetta et al., 2015)	N/A
***gcn5Δ** MATa ade2–1 trp1–1 leu2–3112 his3– 11,15 ura3 can1–100 ssd. gcn5::KanMX4*	(Ornaghi et al., 2005)	N/A
***sgf73Δ** MATa ade2-1 trp1-1 leu2-3 112 his3- 11,15 ura3 can1-100 ssd1. sgf73::His3MX6*	This study	N/A
***spt7Δ** MATa ade2-1 trp1-1 leu2-3 112 his3-11,15 ura3 can1-100 ssd1. spt7::His3MX6*	This study	N/A
***hda1Δ** MATa ade2-1 trp1-1 leu2-3 112 his3- 11,15 ura3 can1-100 ssd1. hda1::His3MX6*	This study	N/A
***gcn5Δhda1Δ** MATa ade2-1 trp1-1 leu2-3 112 his3-11,15 ura3 can1-100 ssd1. gcn5::KanMX4 hda1::His3MX6*	This study	N/A
***bre1Δ** MATa ade2–1 trp1–1 leu2–3112 his3– 11,15 ura3 can1–100 ssd. bre1::KanMX6*	This study	N/A
***ubp8Δbre1Δ** MATa ade2–1 trp1–1 leu2–3112 his3–11,15 ura3 can1–100 ssd. ubp8::His3MX6 bre1::KanMX6*	This study	N/A
***psh1Δ** MATa ade2–1 trp1–1 leu2–3112 his3– 11,15 ura3 can1–100 ssd. psh1::His3MX6*	(Canzonetta et al., 2015)	N/A
***ubp8Δpsh1Δ** MATa ade2–1 trp1–1 leu2–3112 his3–11,15 ura3 can1–100 ssd. ubp8::His3MX6 psh1::KanMX6*	This study	N/A
Ubp8-myc *MATa ade2–1 trp1–1 leu2–3112 his3–11,15 ura3 can1–100 ssd. Ubp8-9myc-HIS3MX6*	(Canzonetta et al., 2015)	N/A
Gcn5-myc *MATa ade2-1 trp1-1 leu2-3 112 his3-11,15 ura3 can1-100 ssd1. GCN5-9Myc-klTRP1*	(Vernarecci et al., 2008)	N/A
Psh1-myc *MATa ade2-1 trp1-1 leu2-3 112 his3-11,15 ura3 can1-100 ssd1. GCN5-9Myc-klTRP1*	This study	N/A
Ubp8-myc *spt20Δ MATa ade2–1 trp1–1 leu2–3112 his3–11,15 ura3 can1–100 ssd. Ubp8-9myc-HIS3MX6 spt20::KanMX6*	This study	N/A

Gcn5-myc *spt20Δ* MATa ade2-1 trp1-1 leu2-3 112 his3-11,15 ura3 can1-100 ssd1. GCN5-9Myc-klTRP1 *spt20::KanMX6*	This study	N/A
Ubp8-myc *psh1Δ MATa ade2–1 trp1–1 leu2–3112 his3–11,15 ura3 can1–100 ssd. Ubp8-9myc-HIS3MX6 psh1::KanMX6*	This study	N/A
Oligonucleotides		
ACT1 Fw: 5'-ACGTTCCAGCCTTCTACGTTTCCA-3'	Sigma	N/A
ACT1 Rev: 5'-AGTCAGTCAAATCTCTACCGGCCA-3	Sigma	N/A
UBP8 Fw: 5'-GGGTATTCACAACAAGATG-3'	Sigma	N/A
UBP8 Rev: 5'-CAGTATGCACTATGCATTC-3	Sigma	N/A
GCN5 Fw: 5'-CATCTTTCCATGGCTGTCATTA-3'	Sigma	N/A
GCN5 Rev: 5'-GAACTGATGGCACAGAAAACAA-3'	Sigma	N/A
DNAgel1: 5′-CTACTATGGCGGGTGATAAAAACGGGAAGAGCATGCCCATCCATGAGCGTACGCAAT-3′	IDT	N/A

DNAgel2: 5′- GGATGGGCATGCTCTTCCCGAACTCAACT GCCTGGTGATACGATGAGCGTACGCAAT- 3′	IDT	N/A
DNAgel3: 5′- CGTATCACCAGGCAGTTGAGAACATGCGA GGGTCCAATACCGATGAGCGTACGCAAT- 3′	IDT	N/A
DNAgel4: 5′- CGGTATTGGACCCTCGCATGAATTTATCA CCCGCCATAGTAGATGAGCGTACGCAAT- 3′	IDT	N/A
DNAcom1: 5′-ATTGCG-3′	IDT	N/A
DNAcom2: 5′-CGCTCA-3′	IDT	N/A
Software and Algorithms		
ImageLab	Biorad	N/A
Rotor-Gene Q series	Qiagen	N/A

REFERENCES

ABATE, G., BASTONINI, E., BRAUN, K. A., VERDONE, L., YOUNG, E. T. & CASERTA, M. 2012. Snf1/AMPK regulates Gcn5 occupancy, H3 acetylation and chromatin remodelling at S. cerevisiae ADY2 promoter. *Biochim Biophys Acta,* 1819, 419-27.

ABE, Y., SHODAI, T., MUTO, T., MIHARA, K., TORII, H., NISHIKAWA, S., ENDO, T. & KOHDA, D. 2000. Structural basis of presequence recognition by the mitochondrial protein import receptor Tom20. *Cell,* 100, 551-60.

BAEZA, J., SMALLEGAN, M. J. & DENU, J. M. 2015. Site-specific reactivity of nonenzymatic lysine acetylation. *ACS Chem Biol,* 10, 122-8.

BAEZA, J., SMALLEGAN, M. J. & DENU, J. M. 2016. Mechanisms and Dynamics of Protein Acetylation in Mitochondria. *Trends Biochem Sci,* 41, 231-244.

BARLEV, N. A., LIU, L., CHEHAB, N. H., MANSFIELD, K., HARRIS, K. G., HALAZONETIS, T. D. & BERGER, S. L. 2001. Acetylation of p53 activates transcription through recruitment of coactivators/histone acetyltransferases. *Mol Cell,* 8, 1243-54.

BRAGOSZEWSKI, P., WASILEWSKI, M., SAKOWSKA, P., GORNICKA, A., BOTTINGER, L., QIU, J., WIEDEMANN, N. & CHACINSKA, A. 2015. Retro-translocation of mitochondrial intermembrane space proteins. *Proc Natl Acad Sci U S A,* 112, 7713-8.

BROACH, J. R. 2012. Nutritional control of growth and development in yeast. *Genetics,* 192, 73-105.

CANZONETTA, C., LEO, M., GUARINO, S. R., MONTANARI, A., FRANCISCI, S. & FILETICI, P. 2016. SAGA complex and Gcn5 are necessary for respiration in budding yeast. *Biochim Biophys Acta,* 1863, 3160-3168.

CANZONETTA, C., VERNARECCI, S., IULIANI, M., MARRACINO, C., BELLONI, C., BALLARIO, P. &

FILETICI, P. 2015. SAGA DUB-Ubp8 Deubiquitylates Centromeric Histone Variant Cse4. *G3 (Bethesda),* 6, 287-98.

CARMEN, A. A., RUNDLETT, S. E. & GRUNSTEIN, M. 1996. HDA1 and HDA3 are components of a yeast histone deacetylase (HDA) complex. *J Biol Chem,* 271, 15837-44.

CASTEGNA, A., IACOBAZZI, V. & INFANTINO, V. 2015. The mitochondrial side of epigenetics. *Physiol Genomics,* 47, 299-307.

CHAN, C. H., LI, C. F., YANG, W. L., GAO, Y., LEE, S. W., FENG, Z., HUANG, H. Y., TSAI, K. K. C., FLORES, L. G., SHAO, Y., HAZLE, J. D., YU, D., WEI, W., SARBASSOV, D., HUNG, M. C., NAKAYAMA, K. I. & LIN, H. K. 2012. The Skp2-SCF E3 Ligase Regulates Akt Ubiquitination, Glycolysis, Herceptin Sensitivity, and Tumorigenesis. *Cell,* 151, 913-914.

CHATTERJEE, A., SEYFFERTH, J., LUCCI, J., GILSBACH, R., PREISSL, S., BOTTINGER, L., MARTENSSON, C. U., PANHALE, A., STEHLE, T., KRETZ, O., SAHYOUN, A. H., AVILOV, S., EIMER, S., HEIN, L., PFANNER, N., BECKER, T. & AKHTAR, A. 2016. MOF Acetyl Transferase Regulates Transcription and Respiration in Mitochondria. *Cell,* 167, 722-738 e23.

CHEN, J. & SEEMAN, N. C. 1991. Synthesis from DNA of a molecule with the connectivity of a cube. *Nature,* 350, 631.

CHEN, L., WEI, T., SI, X., WANG, Q., LI, Y., LENG, Y., DENG, A., CHEN, J., WANG, G., ZHU, S. & KANG, J. 2013. Lysine acetyltransferase GCN5 potentiates the growth of non-small cell lung cancer via promotion of E2F1, cyclin D1, and cyclin E1 expression. *J Biol Chem,* 288, 14510-21.

CHIMENTI, F., BIZZARRI, B., MACCIONI, E., SECCI, D., BOLASCO, A., CHIMENTI, P., FIORAVANTI, R., GRANESE, A., CARRADORI, S., TOSI, F., BALLARIO, P., VERNARECCI, S. & FILETICI, P. 2009. A novel histone acetyltransferase inhibitor modulating Gcn5

network: cyclopentylidene-[4-(4'-chlorophenyl)thiazol-2-yl)hydrazone. *J Med Chem,* 52, 530-6.

COLLINS, S. R., MILLER, K. M., MAAS, N. L., ROGUEV, A., FILLINGHAM, J., CHU, C. S., SCHULDINER, M., GEBBIA, M., RECHT, J., SHALES, M., DING, H., XU, H., HAN, J., INGVARSDOTTIR, K., CHENG, B., ANDREWS, B., BOONE, C., BERGER, S. L., HIETER, P., ZHANG, Z., BROWN, G. W., INGLES, C. J., EMILI, A., ALLIS, C. D., TOCZYSKI, D. P., WEISSMAN, J. S., GREENBLATT, J. F. & KROGAN, N. J. 2007. Functional dissection of protein complexes involved in yeast chromosome biology using a genetic interaction map. *Nature,* 446, 806-10.

DA CUNHA, F. M., TORELLI, N. Q. & KOWALTOWSKI, A. J. 2015. Mitochondrial Retrograde Signaling: Triggers, Pathways, and Outcomes. *Oxid Med Cell Longev,* 2015, 482582.

DAWSON, T. M. & DAWSON, V. L. 2010. The role of parkin in familial and sporadic Parkinson's disease. *Mov Disord,* 25 Suppl 1, S32-9.

DURCAN, T. M. & FON, E. A. 2015. The three 'P's of mitophagy: PARKIN, PINK1, and post-translational modifications. *Genes Dev,* 29, 989-99.

FUKASAWA, Y., TSUJI, J., FU, S. C., TOMII, K., HORTON, P. & IMAI, K. 2015. MitoFates: improved prediction of mitochondrial targeting sequences and their cleavage sites. *Mol Cell Proteomics,* 14, 1113-26.

GHARPURE, K. M., WU, S. Y., LI, C., LOPEZ-BERESTEIN, G. & SOOD, A. K. 2015. Nanotechnology: Future of Oncotherapy. *Clinical Cancer Research,* 21, 3121-3130.

GLINSKY, G. V. 2005. Death-from-cancer signatures and stem cell contribution to metastatic cancer. *Cell Cycle,* 4, 1171-5.

GRAFF, J. & TSAI, L. H. 2013. Histone acetylation: molecular mnemonics on the chromatin. *Nat Rev Neurosci,* 14, 97-111.

GUAN, K. L. & XIONG, Y. 2011. Regulation of intermediary metabolism by protein acetylation. *Trends Biochem Sci,* 36, 108-16.

HEINICKE, S., LIVSTONE, M. S., LU, C., OUGHTRED, R., KANG, F., ANGIUOLI, S. V., WHITE, O., BOTSTEIN, D. & DOLINSKI, K. 2007. The Princeton Protein Orthology Database (P-POD): a comparative genomics analysis tool for biologists. *PLoS One,* 2, e766.

HENRY, K. W., WYCE, A., LO, W. S., DUGGAN, L. J., EMRE, N. C., KAO, C. F., PILLUS, L., SHILATIFARD, A., OSLEY, M. A. & BERGER, S. L. 2003. Transcriptional activation via sequential histone H2B ubiquitylation and deubiquitylation, mediated by SAGA-associated Ubp8. *Genes Dev,* 17, 2648-63.

HSU, H. E., LIU, T. N., YEH, C. S., CHANG, T. H., LO, Y. C. & KAO, C. F. 2015. Feedback Control of Snf1 Protein and Its Phosphorylation Is Necessary for Adaptation to Environmental Stress. *J Biol Chem,* 290, 16786-96.

HUISINGA, K. L. & PUGH, B. F. 2004. A genome-wide housekeeping role for TFIID and a highly regulated stress-related role for SAGA in Saccharomyces cerevisiae. *Mol Cell,* 13, 573-85.

JAZWINSKI, S. M. 2013. The retrograde response: when mitochondrial quality control is not enough. *Biochim Biophys Acta,* 1833, 400-9.

JIN, S. M., LAZAROU, M., WANG, C., KANE, L. A., NARENDRA, D. P. & YOULE, R. J. 2010. Mitochondrial membrane potential regulates PINK1 import and proteolytic destabilization by PARL. *J Cell Biol,* 191, 933-42.

JIN, S. M. & YOULE, R. J. 2013. The accumulation of misfolded proteins in the mitochondrial matrix is sensed by PINK1 to induce PARK2/Parkin-mediated mitophagy of polarized mitochondria. *Autophagy,* 9, 1750-7.

KIM, S., BENGURIA, A., LAI, C. Y. & JAZWINSKI, S. M. 1999. Modulation of life-span by histone deacetylase genes in Saccharomyces cerevisiae. *Mol Biol Cell,* 10, 3125-36.

KIM, S., OHKUNI, K., COUPLAN, E. & JAZWINSKI, S. M. 2004. The histone acetyltransferase GCN5 modulates the retrograde response and genome stability determining yeast longevity. *Biogerontology,* 5, 305-16.

KINNER, A. & KOLLING, R. 2003. The yeast deubiquitinating enzyme Ubp16 is anchored to the outer mitochondrial membrane. *FEBS Lett,* 549, 135-40.

KOUTELOU, E., HIRSCH, C. L. & DENT, S. Y. 2010. Multiple faces of the SAGA complex. *Curr Opin Cell Biol,* 22, 374-82.

LAVIE, J., DE BELVALET, H., SONON, S., ION, A. M., DUMON, E., MELSER, S., LACOMBE, D., DUPUY, J. W., LALOU, C. & BENARD, G. 2018. Ubiquitin-Dependent Degradation of Mitochondrial Proteins Regulates Energy Metabolism. *Cell Rep,* 23, 2852-2863.

LEE, J. B., PENG, S., YANG, D., ROH, Y. H., FUNABASHI, H., PARK, N., RICE, E. J., CHEN, L., LONG, R., WU, M. & LUO, D. 2012. A mechanical metamaterial made from a DNA hydrogel. *Nat Nanotechnol,* 7, 816-20.

LEE, K. K., SARDIU, M. E., SWANSON, S. K., GILMORE, J. M., TOROK, M., GRANT, P. A., FLORENS, L., WORKMAN, J. L. & WASHBURN, M. P. 2011. Combinatorial depletion analysis to assemble the network architecture of the SAGA and ADA chromatin remodeling complexes. *Mol Syst Biol,* 7, 503.

LEO, M., FANELLI, G., DI VITO, S., TRAVERSETTI, B., LA GRECA, M., PALLADINO, R. A., MONTANARI, A., FRANCISCI, S. & FILETICI, P. 2018. Ubiquitin protease Ubp8 is necessary for S. cerevisiae respiration. *Biochim Biophys Acta Mol Cell Res*.

LIBERTI, M. V. & LOCASALE, J. W. 2016. The Warburg Effect: How Does it Benefit Cancer Cells? *Trends Biochem Sci,* 41, 211-218.

LIU, Y., XU, X. & KUO, M. H. 2010. Snf1p regulates Gcn5p transcriptional activity by antagonizing Spt3p. *Genetics,* 184, 91-105.

LIU, Z. & BUTOW, R. A. 2006. Mitochondrial retrograde signaling. *Annu Rev Genet,* 40, 159-85.

LUIS, M. A.-S. 2008. Nucleic Acids as Therapeutic Agents. *Current Topics in Medicinal Chemistry,* 8, 1379-1404.

MAO, C., SUN, W. & SEEMAN, N. C. 1997. Assembly of Borromean rings from DNA. *Nature,* 386, 137.

MARTINEZ-CERDENO, V., LEMEN, J. M., CHAN, V., WEY, A., LIN, W., DENT, S. R. & KNOEPFLER, P. S. 2012. N-Myc and GCN5 regulate significantly overlapping transcriptional programs in neural stem cells. *PLoS One,* 7, e39456.

MATILAINEN, O., QUIROS, P. M. & AUWERX, J. 2017. Mitochondria and Epigenetics - Crosstalk in Homeostasis and Stress. *Trends Cell Biol,* 27, 453-463.

MENZIES, K. J., ZHANG, H., KATSYUBA, E. & AUWERX, J. 2016. Protein acetylation in metabolism - metabolites and cofactors. *Nat Rev Endocrinol,* 12, 43-60.

MONTANARI, A., BESAGNI, C., DE LUCA, C., MOREA, V., OLIVA, R., TRAMONTANO, A., BOLOTIN-FUKUHARA, M., FRONTALI, L. & FRANCISCI, S. 2008. Yeast as a model of human mitochondrial tRNA base substitutions: investigation of the molecular basis of respiratory defects. *RNA,* 14, 275-83.

MOORE, D. S. 2017. Behavioral epigenetics. *Wiley Interdiscip Rev Syst Biol Med,* 9.

NISHIKAWA, M., OGAWA, K., UMEKI, Y., MOHRI, K., KAWASAKI, Y., WATANABE, H., TAKAHASHI, N., KUSUKI, E., TAKAHASHI, R., TAKAHASHI, Y. & TAKAKURA, Y. 2014. Injectable, self-gelling, biodegradable, and immunomodulatory DNA hydrogel for antigen delivery. *Journal of Controlled Release,* 180, 25-32.

ORNAGHI, P., ROTILI, D., SBARDELLA, G., MAI, A. & FILETICI, P. 2005. A novel Gcn5p inhibitor represses cell growth, gene transcription and histone acetylation in budding yeast. *Biochem Pharmacol,* 70, 911-7.

OTTERSTEDT, K., LARSSON, C., BILL, R. M., STAHLBERG, A., BOLES, E., HOHMANN, S. & GUSTAFSSON, L. 2004. Switching the mode of metabolism in the yeast Saccharomyces cerevisiae. *EMBO Rep,* 5, 532-7.

PARK, C. W. & RYU, K. Y. 2014. Cellular ubiquitin pool dynamics and homeostasis. *BMB Rep,* 47, 475-82.

PENG, W., TOGAWA, C., ZHANG, K. & KURDISTANI, S. K. 2008. Regulators of cellular levels of histone acetylation in Saccharomyces cerevisiae. *Genetics,* 179, 277-89.

PRAY-GRANT, M. G., SCHIELTZ, D., MCMAHON, S. J., WOOD, J. M., KENNEDY, E. L., COOK, R. G., WORKMAN, J. L., YATES, J. R., 3RD & GRANT, P. A. 2002. The novel SLIK histone acetyltransferase complex functions in the yeast retrograde response pathway. *Mol Cell Biol,* 22, 8774-86.

QUIROS, P. M., MOTTIS, A. & AUWERX, J. 2016. Mitonuclear communication in homeostasis and stress. *Nat Rev Mol Cell Biol,* 17, 213-26.

RADKE, S., CHANDER, H., SCHAFER, P., MEISS, G., KRUGER, R., SCHULZ, J. B. & GERMAIN, D. 2008. Mitochondrial protein quality control by the proteasome involves ubiquitination and the protease Omi. *J Biol Chem,* 283, 12681-5.

ROTHBART, S. B. & STRAHL, B. D. 2014. Interpreting the language of histone and DNA modifications. *Biochim Biophys Acta,* 1839, 627-43.

RUSSO, J., TAVARES, J. M., TEIXEIRA, P. I. C., TELO DA GAMA, M. M. & SCIORTINO, F. 2011. Reentrant Phase Diagram of Network Fluids. *Physical Review Letters,* 106, 085703.

SCOTT, I., WANG, L., WU, K., THAPA, D. & SACK, M. N. 2018. GCN5L1/BLOS1 Links Acetylation, Organelle Remodeling, and Metabolism. *Trends Cell Biol,* 28, 346-355.

SCOTT, I., WEBSTER, B. R., LI, J. H. & SACK, M. N. 2012. Identification of a molecular component of the

mitochondrial acetyltransferase programme: a novel role for GCN5L1. *Biochem J,* 443, 655-61.

SEEMAN, N. C. 2003. DNA in a material world. *Nature,* 421, 427.

SHAHBAZI, M.-A., BAULETH-RAMOS, T. & SANTOS, H. A. 2018. DNA Hydrogel Assemblies: Bridging Synthesis Principles to Biomedical Applications. *ADVANCED THERAPEUTICS,* 1, 1800042.

SHI, L. & TU, B. P. 2015. Acetyl-CoA and the regulation of metabolism: mechanisms and consequences. *Curr Opin Cell Biol,* 33, 125-31.

SINGER, A., MARKOUTSA, E., LIMAYEM, A., MOHAPATRA, S. & MOHAPATRA, S. S. 2018. Nanobiotechnology Medical Applications: Overcoming Challenges Through Innovation. 2, 146.

SIRRENBERG, C., BAUER, M. F., GUIARD, B., NEUPERT, W. & BRUNNER, M. 1996. Import of carrier proteins into the mitochondrial inner membrane mediated by Tim22. *Nature,* 384, 582-5.

TLUSTY, T. & SAFRAN, S. A. 2000. Defect-Induced Phase Separation in Dipolar Fluids. *Science,* 290, 1328-1331.

UM, S. H., LEE, J. B., PARK, N., KWON, S. Y., UMBACH, C. C. & LUO, D. 2006. Enzyme-catalysed assembly of DNA hydrogel. *Nature Materials,* 5, 797.

VERNARECCI, S., ORNAGHI, P., BAGU, A., CUNDARI, E., BALLARIO, P. & FILETICI, P. 2008. Gcn5p plays an important role in centromere kinetochore function in budding yeast. *Mol Cell Biol,* 28, 988-96.

VOGELAUER, M., WU, J., SUKA, N. & GRUNSTEIN, M. 2000. Global histone acetylation and deacetylation in yeast. *Nature,* 408, 495-8.

WANG, D., HU, Y., LIU, P. & LUO, D. 2017. Bioresponsive DNA Hydrogels: Beyond the Conventional Stimuli Responsiveness. *Accounts of Chemical Research,* 50, 733-739.

WANG, L. & DENT, S. Y. 2014. Functions of SAGA in development and disease. *Epigenomics,* 6, 329-39.

WIEDEMANN, N. & PFANNER, N. 2017. Mitochondrial Machineries for Protein Import and Assembly. *Annu Rev Biochem,* 86, 685-714.

WILSON, M. A., KOUTELOU, E., HIRSCH, C., AKDEMIR, K., SCHIBLER, A., BARTON, M. C. & DENT, S. Y. 2011. Ubp8 and SAGA regulate Snf1 AMP kinase activity. *Mol Cell Biol,* 31, 3126-35.

WYCE, A., XIAO, T., WHELAN, K. A., KOSMAN, C., WALTER, W., EICK, D., HUGHES, T. R., KROGAN, N. J., STRAHL, B. D. & BERGER, S. L. 2007. H2B ubiquitylation acts as a barrier to Ctk1 nucleosomal recruitment prior to removal by Ubp8 within a SAGA-related complex. *Mol Cell,* 27, 275-88.

YANG, W. L., WANG, J., CHAN, C. H., LEE, S. W., CAMPOS, A. D., LAMOTHE, B., HUR, L., GRABINER, B. C., LIN, X., DARNAY, B. G. & LIN, H. K. 2009. The E3 ligase TRAF6 regulates Akt ubiquitination and activation. *Science,* 325, 1134-8.

YANG, X. J. & SETO, E. 2008. The Rpd3/Hda1 family of lysine deacetylases: from bacteria and yeast to mice and men. *Nat Rev Mol Cell Biol,* 9, 206-18.

ZHANG, X. Y., VARTHI, M., SYKES, S. M., PHILLIPS, C., WARZECHA, C., ZHU, W., WYCE, A., THORNE, A. W., BERGER, S. L. & MCMAHON, S. B. 2008. The putative cancer stem cell marker USP22 is a subunit of the human SAGA complex required for activated transcription and cell-cycle progression. *Mol Cell,* 29, 102-11.

ZHANG, Y. & SEEMAN, N. C. 1994. Construction of a DNA-Truncated Octahedron. *Journal of the American Chemical Society,* 116, 1661-1669.

PUBLICATIONS

"Mitochondria and metabolism: the role of SAGA complex in budding yeast respiration":
CANZONETTA, C., LEO, M., GUARINO, S.R., MONTANARI, A., FRANCISCI, S., FILETICI, P. 2016. SAGA complex and Gcn5 are necessary for respiration in budding yeast. BBA Molecular Cell Research 1863, 3160

LEO, M., FANELLI, G., DI VITO, S., TRAVERSETTI, B., LA GRECA, M., PALLADINO, R.A., MONTANARI, A., FRANCISCI, S., FILETICI, P. 2018. Ubiquitin protease Ubp8 is necessary for S. cerevisiae respiration. BBA Molecular Cell Research 1865, 1491

MONTANARI, A., LEO, M., DE LUCA, V., FILETICI, P., FRANCISCI S. Gcn5 histone acetyltransferase is present in the mitoplasts. 2019. Biology Open. ARTICLE IN PRESS.

"Re-entrant DNA gels":
BOMBOI, F., ROMANO, F., LEO, M., FERNANDEZ-CASTANON, J., CERBINO, R., BELLINI, T., BORDI, F., FILETICI, P., SCIORTINO, F. 2016. Re-entrant DNA gels. Nature Communications 7, 13191

Other publications:
COCCO, E., LEO, M., CANZONETTA, C., DI VITO, S., MAI, A., ROTILI, D., DI NAPOLI, A., VECCHIONE, A., DE NUNZIO, C., FILETICI, P., STOPPACCIARO, A. 2018. p300 and H3AcK18/H3AcK14 levels are prognostic markers for kidney ccRCC tumor aggressiveness and target of KAT inhibitor CPTH2. Clinical Epigenetics 10, 44

AKNOWLEDGMENTS